COMPARATIVE STUDIES OF
SOME SIMPLE VISCOELASTIC THEORIES

by

R. I. Tanner

Division of Engineering, Brown University

Providence, R. I.

September 1967

Synopsis

Some current simple integral theories of the Lodge type are compared in simple shearing, small sinusoidal shearing, combined simple and sinusoidal shearing, cessation and start of simple shearing, finite amplitude sinusoidal shearing and simple elongational motions. Of these only the recently proposed network-rupture theory shows a realistic response in elongational flows; in the other flows it behaves a little better than other recent integral models in experimental comparisons with data from polyisobutylene-cetane solutions.

1. Integral-Type Constitutive Equations

Recently great interest has been shown in integral, as opposed to differential[1], types of simple rheological constitutive equations. Certain instability problems and general awkwardness[2] in use for some very simple flows make differential models unattractive to the author and they will not be discussed further. A survey of some earlier integral type equations and a discussion of some of their drawbacks has already been given elsewhere[3]. Here certain recently proposed integral models are compared for performance in simple flows.

The upsurge in interest in integral models seems to be due in part to the exposition by Lodge[4], who shows the striking results obtained from a constitutive relation of the form

$$\underline{\underline{T}} + p\underline{\underline{I}} = \int_{-\infty}^{t} N(t - t')\, \underline{\underline{S}}(t')\, dt' \qquad (1)$$

Here $\underline{\underline{T}}$, $\underline{\underline{I}}$ and $\underline{\underline{S}}$ are the stress, unit and (finite) strain matrices respectively, p is the pressure, and $N(t - t')$ is the memory function reflecting the number of network junctions that were created in the fluid at time t' in the past and which still persist at the present time t. $\underline{\underline{S}}(t')$ is the strain of an element at time t' relative to the present time t as reference; a useful form of $\underline{\underline{S}}(t')$ (due to Lodge; see ref. 1.) is

$$\underline{\underline{S}} = (1 + \varepsilon)\, \underline{\underline{B}} + \varepsilon \underline{\underline{C}} \qquad (2)$$

where ε is a number and $\underline{\underline{B}}$ and $\underline{\underline{C}}$ are the Finger[5] and Green[6] strain matrices respectively. In a simple shearing flow where the velocity vector $\underline{v}$ is given by

$$\underline{v} = (\gamma y, 0, 0) \qquad (3)$$

with γ as the shearing rate, it is easily shown[4] that ε governs the

ratio of the second to the first normal stress difference. Thus, in simple shearing, with $\underline{v}$ given by equation (2), we have

$$\varepsilon = \frac{t_{yy} - t_{zz}}{t_{xx} - t_{yy}} \tag{4}$$

where t_{xx}, etc. are the components of $\underline{\underline{T}}$. The main difficulty with equation (1) is that it predicts a constant viscosity in simple shearing. We find[4]

$$t_{xy} = \gamma \int_0^\infty \tau N(\tau)\, d\tau \tag{5}$$

Several suggestions have been advanced to overcome this problem. Bogue and Doughty[7] discuss various integral models and Bogue[8] suggests a modification whereby the kernel $N(\tau)$ becomes a function of the flow history. It is supposed that the memory function $N(\tau)$ has a discrete-spectrum form, so that

$$N(\tau) = \sum_n \frac{a_n}{\lambda_n^2}\, e^{-\tau/\lambda_n} \tag{6}$$

where the a_n are constants with the dimensions of viscosity and the λ_n are time constants. Bogue[8] then suggests that the flow modifies the λ_n according to the rule

$$\frac{1}{\lambda_{eff}} = \frac{1}{\lambda_n} + aK(s) \tag{7}$$

where λ_{eff} is the effective time constant during flow, $K(s)$ is a mean shear rate over the past history, and a is a constant. For most simple flows this yields very complicated expressions; for simple shearing one obtains the viscosity function $\eta_s(\gamma)$ as

$$\eta_s(\gamma) = \int_0^\infty \frac{H d\lambda}{1 + a|\gamma|\lambda} \tag{8}$$

where $H(\lambda)$ is the relaxation spectrum. $H(\lambda)$ is related to $N(\tau)$ by the

Laplace transform rule[9], i.e.

$$N(\tau) = \int_0^\infty \frac{H(\lambda)e^{-\tau/\lambda}}{\lambda^2}\, d\lambda \qquad (9)$$

Bird and Macdonald[10] suggest replacing the kernel of (1) by the form

$$N(t-t') = (\eta_o/\sum_{n=1}^{\infty} \lambda_n) \sum_{n=1,2--}^{\infty} \lambda_n^{-1} [1+2II(t')c^2\lambda_n^2]^{-1} \exp[(-t+t')/\lambda_n] \qquad (10)$$

where $II(t')$ is the second invariant of the rate of deformation matrix $\underline{\underline{D}} \left(\equiv \frac{1}{2}\left(\frac{\partial v_i}{\partial x_j} + \frac{\partial v_j}{\partial x_i}\right)\right)$, the λ_n are time constants, η_o is the zero-shear-rate viscosity and c is a constant. The time constants are related to a master time constant λ by the equation

$$\lambda_n = \lambda/n^\alpha \qquad (11)$$

where α is a constant. The complexity of (10) and (11) is more apparent than real and the choice of λ_n is guided by the Rouse[11] molecular theory, which holds for sharp molecular weight distributions. For wide distributions of molecular weight the essential features of (10) could also be retained with arbitrary time constant distributions of the form (6) but containing the extra factors depending on $II(t')$. A result of this theory for simple shearing may be written

$$\eta_s(\gamma) = \int_0^\infty \frac{H d\lambda}{1 + c^2\lambda^2\gamma^2} \qquad (12)$$

which is very similar to eqn. (8). In other flows the Bird-Macdonald[10] modification is much more tractable than Bogue's[8] and the latter does not seem to have any advantages; hence it will not be discussed further.

Kaye[12] suggests that the kernel N be modified to allow for variation of the memory function with stress. This leads to an implicit

equation for the stress components and not surprisingly he confines his attention to simple shearing. Tanner and Simmons[2] introduce the idea of network rupture at a given critical strain magnitude. When some measure of $\underline{\underline{S}}(t')$ in a linkage exceeds the critical magnitude the network linkage ruptures and does not contribute further to the stress in the flowing polymer. Molecular aspects of the rupture hypothesis have been discussed elsewhere[13]; in the present paper this scheme is compared, where possible, with the Bird-Macdonald[10] equation and with experiments in steady and unsteady shearing motions and in steady elongational flow.

2. A Network-Rupture Theory

An explicit form of the network-rupture theory has been given previously[2]. Recapitulating, it is supposed that the critical strain magnitude is reached when

$$\mathrm{tr}\ \underline{\underline{B}}(t') = B^2 \tag{13}$$

where B is a number expected to be[13] of order 1-10. Equation (13) defines a time t'_c which gives the age of the oldest surviving junctions in simple flows (e.g. viscometric and elongational flows). In simple shearing, two neighbouring points in the flow move apart monotonically and eqn. (13) becomes

$$\gamma^2(t - t'_c)^2 = B^2 \tag{14}$$

Thus the age τ_R $(= t - t'_c)$ of the oldest surviving junction is, from (14), given by

$$\tau_R = B/|\gamma| \tag{15}$$

Henceforward we shall drop the modulus sign from (15) understanding γ to be positive. It is easily shown that the result of the rupture hypothesis is to replace the infinite limit in equation (1) by $t - \tau_R$; the results for

the steady-shear viscosity ($\eta_s(\gamma)$) and the first normal stress difference $t_{xx} - t_{yy}$ then follow readily; the second normal stress difference is then found from equation (4). The results are

$$\eta_s(\gamma) = \sum_n a_n[1 - (1 + \Gamma_n^{-1}) \exp - (1/\Gamma_n)] + \eta_\infty \qquad (16)$$

$$\frac{t_{xx} - t_{yy}}{\gamma^2} = \sum_n 2a_n\lambda_n[1 - (1 + \Gamma_n^{-1} + \frac{1}{2}\Gamma_n^{-2}) \exp - (1/\Gamma_n)] \qquad (17)$$

where $\Gamma_n = \lambda_n\gamma/B$. The factor η_∞ in equation (16) is the limiting viscosity at large shear rate and this is not included in equation (6)[2]. The value of $\eta_s(\gamma)/\eta_o$ for these two models is shown in Fig. 1 for a single time constant, $n = 1$, with $a_n = \eta_o$, $\eta_\infty = 0$. Curves A and B represent equations (16) and (12) respectively. The value of c in equation (10) has been set so that

$$c = 1.68/B \qquad (18)$$

then a direct comparison can be made between the curves A and B in fig. 1 since the curves coincide at $\eta/\eta_o = 0.5$. Clearly either curve will give satisfactory results in fitting experimental viscosity curves. For a 5.39% polyisobutylene-cetane solution* Simmons[19,20] has measured both the dynamic and steady shear viscosities. Figure 2 shows the dynamic viscosity-frequency curve which has been fitted by the discrete spectrum of Table I. The fit is clearly sufficiently accurate; probably fewer time constants could be used. A choice of $B = 2.0$, 2.4 and 3.5 as in Table I fits the shear curve almost exactly, Fig. 2.

---

*Viscosity average M.W. of 1.0×10^6 ; the cetane was of 99% minimum purity. Dr. H. Markovitz of the Mellon Institute kindly donated the polyisobutylene sample.

TABLE I

Fitted Spectrum for 5.39% p.i.b./cetane solution at 25°C

n	λ_n(sec.)	a_n (poise)	B
1	0.7	0.01	2.0
2	0.3	0.7	2.0
3	0.14	1.15	2.0
4	0.08	2.7	2.0
5	0.04	1.6	2.4
6	0.018	1.5	2.4
7	0.01	1.0	2.4
8	0.007	0.9	2.4
9	0.004	0.8	3.5
10	0.002	0.8	3.5
11	0.0015	0.5	3.5
12	0.0008	0.5	3.5

η_∞ = 0.3 poise.

If the single value of $B = 2.4$ is chosen the result is almost indistinguishable from the Bird-Macdonald model with $c = 0.7$. In both cases the spectrum of Table I has been used. Thus either model is satisfactory here. Figure 1 also shows the values of $(t_{xx} - t_{yy})/2\gamma^2\eta_o\lambda$ for a single time constant. Curve C represents equation (17) and the Bird-Macdonald model is again represented by Curve B. Figure 3 shows the computed normal stress curves for the spectrum of Table I, experimental data obtained in a Couette viscometer, and the normal stress data af Markovitz and Brown.[14] The small difference between our 5.4% data and the data of Markovitz and Brown[14] for a 5.39% polyisobutylene-cetane solution of slightly higher viscosity (η_o - 18 poise) is noted. It is clear that equations (17) and the corresponding Bird-Macdonald expression diverge equally from the data at higher shear rates. Equation (17) is better at moderate shear rates; both diverge from the results of Markovitz and Brown[14] at low shear rates. The experimental dynamic elasticity $G'(\omega)$ and that calculated from the spectrum is also shown in Fig. 3. It does not apeear that the experimental data will satisfy the relation

$$\lim_{\gamma \to 0} \left| \frac{t_{xx} - t_{yy}}{\gamma^2} \right| = \lim_{\omega \to 0} \left| 2 \frac{G'(\omega)}{\omega^2} \right| \qquad (19)$$

predicted by all simple fluid theories[15]; much better agreement would be obtained without the factor 2 in (19). This has been noted previously[16].

The constancy of ϵ may also be tested. Figure 4 shows experimental results for the two samples of 5.4% polyisobutylene-cetane solution discussed in Fig. 3. The values of ϵ are much higher than those observed in some aqueous solutions[17]. A mean value of ϵ of around 0.5-0.6 seems to be indicated for higher shear rates. In conclusion, it appears that either of the two simple integral models discussed above can represent

the basic viscometric functions and the infinitesimal strain results with reasonable accuracy. Overall the rupture model seems slightly superior. We now examine some non-viscometric motions.

3. Combined Sinusoidal and Simple Shearing

The response of a sample undergoing simple shearing to a superposed small sinusoidal shear is of interest, for example, in flow stability calculations for viscoelastic fluids. Two basic situations are of interest; either the superposed small shear is parallel to or transverse to the simple shearing. We denote these possibilities by subscripts p and t respectively. Because of the linearity of the added infinitesimal motions no loss in generality arises from considering the two cases separately. For finite-amplitude superposed motions it would not in general be possible to split the response this way.[4] Inertia forces will be neglected in this and the following sections.

For the transverse case, for infinitesimal sinusoidal amplitudes, we find[2], for the network rupture theory with a single time constant

$$\frac{\eta_t}{\eta_o}(\gamma,\omega) = (1+\Lambda^2)^{-1}\left[1+\left(\Lambda^{-1}\sin\Lambda/\Gamma+\cos\Lambda/\Gamma\right)e^{-1/\Gamma}\right] \qquad (20)$$

where $\Lambda = \lambda\omega$, $\Gamma = \gamma\lambda/B$. For the Bird-Macdonald theory[18] we find, with $c = 1.68/B$,

$$\frac{\eta_t}{\eta_o} = \left[(1+\Lambda^2)(1+2.82\Gamma^2)\right]^{-1} \qquad (21)$$

For $\Gamma = 0, 1/2, 1, 2$ these results are compared in Fig. 5. Similar curves for $\Gamma = 0, 1$ are shown in Fig. 6 for the dynamic elasticity, $G_t'(\gamma,\omega)$. The relevant expressions are[2,18]

$$\frac{G_t'\lambda}{\eta_o} = [1 + \Lambda^2]^{-1}\left[\Lambda^2 + (\cos\Lambda/\Gamma - \Lambda\sin\Lambda/\Gamma - \Lambda^2 - 1)\, e^{-1/\Gamma}\right] \qquad (22)$$

$$\frac{G_t''\lambda}{\eta_o} = \Lambda^2[(1 + \Lambda^2)(1 + 2.82\Gamma^2)]^{-1} \qquad (23)$$

Experimental results obtained by Simmons[19] for the 5.4% p.i.b. cetane solution discussed previously are shown in Figs. 7 and 8. Although one might consider from figs. 5 and 6 that the models differ greatly in such a flow it turns out that they are quite similar. Comparisons with experiments[19] are shown in Figs. 7 and 8. In both cases the values of Table I and $c = 0.7$ have been used in the calculations. The network-rupture model appears to be slightly better in viscosity predictions; at low frequencies the Bird-Macdonald model predicts $G_t'(\gamma,\omega)$ better in most cases; at high frequencies the rupture theory is considerably superior.

It is obvious that another anomaly is present here. For all isotropic fluids we expect

$$\lim_{\omega\to 0} \eta_t(\gamma,\omega) = \eta_s(\gamma) \qquad (24)$$

This condition is not fulfilled as is clear from Fig. 7. It is believed that the experiments are sufficiently accurate[19,20] (maximum of about 5% error) and it appears that the cause of the discrepancy must lie in our inability to reach a sufficiently low frequency for eqn. (24) to hold rigorously. However, the persistent disagreement down to frequencies much below the principal relaxation times is to be noted. Further exploration of this point is being made; at the moment we note[2,19] that all concentrations of polyisobutylene-cetane samples gave a similar effect; for a 1.5% carboxymethylcellulose-distilled water sample (fig. 9 and 10) the effect is less

pronounced but still visible.

The parallel case is a little more complex and there is more direct interaction between the sinusoidal motion and the main shearing. Some, but not all, of this interaction can be illustrated by considering a completely inelastic fluid with a variable viscosity. Suppose

$$\underline{\underline{T}} = 2\underline{\underline{D}}\eta(2\mathrm{tr}\underline{\underline{D}}^2) \tag{25}$$

In parallel superposition the interesting component of $\underline{\underline{T}}$ is t_{xy}. For $\underline{\underline{D}}$ we have $d_{xy} = \frac{1}{2}\frac{\partial u}{\partial y}$; thus $2\mathrm{tr}D^2 = \left(\frac{\partial u}{\partial y}\right)^2$. If the velocity component u is of the form

$$u = \gamma y + \hat{a}\omega y \sin\omega t$$

where $\hat{a}$ is the maximum (small) sinusoidal strain, we find

$$t_{xy} \equiv t^{\circ}_{xy} + \hat{a}t'_{xy} = \gamma\eta(\gamma^2) + \left[\gamma\frac{\partial\eta}{\partial\gamma}\Big|_{\hat{a}=0} + \eta(\gamma^2)\right]\hat{a}\omega\sin\omega t + O(\hat{a}^2) \tag{26}$$

Thus the "mean viscosity", t°_{xy}/γ is altered only to order $O(\hat{a}^2)$, while the effective dynamic viscosity $\eta'_p(\equiv t'_{xy}/\omega)$ becomes

$$\eta'_p = \eta + \frac{\partial\eta}{\partial \ell n\gamma} + O(\hat{a}) \tag{27}$$

The error term is thus proportional to the sinusoidal amplitude. In contrast, for the transverse case we find $2\mathrm{tr}D^2 = \gamma^2 + \hat{a}^2\omega^2\sin^2\omega t$ and

$$\left.\begin{aligned} t^{\circ}_{xy}/\gamma &= \eta(\gamma^2) + O(\hat{a}^2) \\ \eta' &= \eta(\gamma^2) + O(\hat{a}^2) \end{aligned}\right\} \tag{28}$$

Thus one may expect that amplitude effects will cause least disturbance to the measurements in the transverse configuration.

In Figs. 7-10 the value of $\hat{a}$ was between 0.04 and 0.08 and no significant amplitude effects were noted.[19]

Several reports of parallel superposition have appeared recently[21-23] and analyses of this case have been given[10,24]. Here the response for a single relaxation time with the rupture model is given. This illustrates some of the points made above.

From ref. 4 we find the S_{xy} component of $\underline{\underline{S}}$ to be

$$S_{xy} = \gamma(t - t') + \hat{a}(\sin\omega t - \sin\omega t')$$

$$\text{tr } \underline{\underline{B}} = B_{xy}^2 = \gamma^2(t - t')^2 + 2\hat{a}\gamma(t - t')(\sin\omega t - \sin\omega t') + 0(\hat{a}^2)$$

Setting $\text{tr } \underline{\underline{B}} = B^2$ we find the rupture time τ_R is given by

$$\tau_R = \frac{B}{\gamma} - \frac{\hat{a}}{\gamma}\left\{\sin\omega t - \sin\omega\left(t - \frac{B}{\gamma}\right)\right\} + 0(\hat{a}^2)$$

Hence, substituting in equation (1) we find

$$\frac{t^o_{xy}}{\gamma\eta_o} = 1 - (1 + B/\lambda\gamma)\exp(-B/\lambda\gamma) + 0(\hat{a}^2) \qquad (29)$$

and

$$G'_p(\omega,\gamma) = G'_t(\omega,\gamma) - \frac{B\eta_o}{\gamma\lambda^2}(1 - \cos\omega B/\gamma)\exp(-B/\lambda\gamma) + 0(\hat{a}) \qquad (30)$$

$$G''_p(\omega,\gamma) \equiv \omega\eta'_p(\omega,\gamma) = G''_t(\omega,\gamma) - \frac{B\eta_o}{\gamma\lambda^2}\sin\omega B/\gamma\exp(-B/\lambda\gamma) + 0(\hat{a}) \qquad (31)$$

In both (30) and (31) the expressions may become negative; this also occurs in the Bird-Macdonald model[10]. Figure 11 shows values of $|G'_p|\lambda/\eta_o$; for $\lambda\omega < 1$, 1.4, G'_p is negative for the rupture model and the Bird-Macdonald model respectively. This extraordinary behaviour is masked with many time

constants and has not been observed to the author's knowledge. The experiments of Osaki et al[21,22] unfortunately do not cover wide enough ranges of variables accurately to inspect the type of result given by equation (24). In the experiments of Booij[23] the values of dynamic viscosity $\eta_p(\dot{\gamma},\omega)$ are considerably below the value of $\eta_s(\dot{\gamma})$ for the lowest frequencies; this is predicted by equation (31). In summary, we note that the superposition of small-amplitude and simple shearing gives some interesting results and that the transverse configuration is the least complex. In addition, it is clear that both integral theories give reasonable predictions here; perhaps the network rupture theory is a little better overall. The striking reduction in fluid elasticity due to shearing is obvious; in references 2, 13 and 22 the changes of the relaxation spectra $H(\lambda)$ due to shearing are discussed.

4. Finite Amplitude Unsteady Shearing Motions

In this section we investigate inertialess shearing motions in which the velocity field is of the form (3) but where the shear rate is a function of time. It must be said that the dismissal of inertia in such flows may often be unrealistic and care may be necessary in experimental comparisons.

A popular test[16] has been the study of the decay of shearing stresses after suddenly stopping a steady shear flow. In this case we find that the rupture and Bird-Macdonald models give practically identical results. It is easily shown that for discrete relaxation times they both give the result

$$\frac{t_{xy}}{\dot{\gamma}} = \sum_n a_n e^{-t/\lambda_n} f(\lambda_n \dot{\gamma}) \qquad (32)$$

where $f(\lambda_n\dot{\gamma})$ gives the steady-shear viscosity ratio η_s/η_o for a single relaxation time λ_n (eqn. (16) for the rupture model). Except with the single relaxation time, the normal stress differences relax more slowly than the shear stress.[4] Despite its popularity

we see that the stop-shear test is useless for distinguishing between reasonable non-linear theories. The start-shear test is much more informative and this is now discussed.

In the start-shear problem it is clear that no linkages can rupture before the fluid has been strained a certain amount. When shearing does commence, we have

$$\left.\begin{aligned} S_{xy} &= \gamma(t - t'),\ t' > 0 \\ &= \gamma t \qquad\quad 0 > t' \end{aligned}\right\} t > 0 \tag{33}$$

For $t < 0$, $\underline{\underline{S}} = \underline{\underline{0}}$. Hence (1) becomes[4]

$$t_{xy} = \int_0^t N\,\gamma(t - t')dt' + \gamma t \int_{t-\tau_R}^0 N(t - t')\,dt' \tag{34}$$

To find τ_R we calculate $\mathrm{tr}\,\underline{\underline{B}}$, which is then equated to B^2. Hence, using the expression for negative t' in (33), we find

$$\gamma t = B \tag{35}$$

and thus no rupture occurs before a time B/γ has elapsed after starting; in this region τ_R is infinite and Lodge's result[4] is recovered. Immediately after this time ($t = B/\gamma$) all the surviving old linkages rupture and a state of steady shearing is instantly reached. This occurs because the memory time now goes back a distance B/γ; for $t > B/\gamma$ the second integral in (34) vanishes while the first integral yields the result (16). Evaluating the integrals (34) we find, in terms of the "transient" viscosity t_{xy}/γ,

$$\left.\begin{aligned} \frac{t_{xy}}{\gamma\eta_S(\gamma)} = \frac{\eta_S(t,\gamma)}{\eta_S(\infty,\gamma)} &= \frac{1 - e^{-t/\lambda}}{1-(1+\Gamma^{-1})e^{-1/\Gamma}} \quad \text{for } \frac{B}{\gamma} > t \\ &= 1 \quad \text{for } t > B/\gamma \end{aligned}\right\} \tag{36}$$

This expression is for a single relaxation time λ. It is easily shown that the Bird-Macdonald model gives the corresponding result

$$\frac{\eta_S(t,\gamma)}{\eta_S(\gamma)} = 1 - e^{-t/\lambda}\,(1 - c^2\lambda\gamma^2 t) \tag{37}$$

Choosing $c = 1.68/B$ we compare these expressions in Fig. 12. The rupture model shows a much quicker return after overshoot and this seems to be

characteristic of experiments[25]. Unfortunately it is not possible to compare with the data of reference 25 because the dynamic measurements are not given. One expects that this test will provide a means for estimating the distribution of rupture strains by looking at the peak shape; certainly one expects rounder peaks than those predicted for a constant rupture strain. It is ~~expected~~ hoped that this type of experiment will be quite useful in distinguishing between theories.

As a final example of this type of motion we consider a sinusoidal shearing motion of finite amplitude, again neglecting inertia. Philippoff[26] has reported some experiments on this type of motion in which inertia may have played a negligible role. Suppose that the variable shear is sinusoidal, i.e.

$$\gamma = -\hat{a}\omega\sin\omega t \tag{38}$$

Then we find that S_{xy} has the value

$$S_{xy}(t') = \hat{a}\{\cos\omega t - \cos\omega t'\} \tag{39}$$

and $\mathrm{tr}\,\underline{\underline{B}}$ is S_{xy}^2. Hence rupture occurs when $S_{xy} = B$. From equation (39) and Fig. 13a we see that no rupture ever occurs if $B > 2\hat{a}$. In this case the problem is linear and the value of t_{xy} is given, for n discrete relaxation times, by

$$\frac{t_{xy}}{\hat{a}\omega} = \sum_n a_n \frac{\Lambda_n \cos\theta}{1+\Lambda_n^2} - \sum_n a_n \frac{\sin\theta}{1+\Lambda^2} \qquad \left(\hat{a} < \frac{B}{2}\right) \tag{40}$$

where $\theta = \omega t$, $\Lambda_n = \omega\lambda_n$. For $\hat{B} > \hat{a} > B/2$ we have rupture occurring as shown in the shaded parts of fig. 13b. The unshaded areas continue to contribute to the stresses in the medium and their total effect is expressed as a series which can be summed readily. The final expression for $t_{xy}/\hat{a}\omega$

is given by

$$\frac{t_{xy}}{\hat{a}\omega} = -\cos\theta \sum_n \frac{a_n \exp-(\pi/2+\theta)/\Lambda_n}{\Lambda_n \sinh \pi/2\Lambda_n}\left\{\sinh\xi/\Lambda_n + H(\theta-\pi+\xi)\sinh\frac{\alpha}{\Lambda_n}\left[e^{\pi/\Lambda_n}-1\right]\right\}$$

$$-\sin\theta \sum_n \frac{a_n}{1+\Lambda_n^2} + \cos\theta \sum_n \frac{a_n\Lambda_n}{1+\Lambda_n^2} -$$

$$-\sum_n \frac{a_n \exp-(\pi/2+\theta)/\Lambda_n}{\Lambda_n(1+\Lambda_n^2)\cosh \pi/2\Lambda_n}\left\{\begin{array}{l}\Lambda_n\sin\xi\cosh\xi/\Lambda_n + \cos\xi\sinh\xi/\Lambda_n \\ -H(\theta-\pi+\xi)(e^{\pi/\Lambda_n}+1)\left[\begin{array}{l}\sinh\frac{\alpha}{\Lambda_n}\cos\alpha \\ +\Lambda_n\cosh\frac{\alpha}{\Lambda_n}\sin\alpha\end{array}\right]\end{array}\right\} \quad (41)$$

where $H(x)$ is the Heaviside function, equal to unity for $x > 0$, zero for $0 > x$,

$$\cos\xi = \frac{B}{\hat{a}} - 1 \quad (42)$$

$$\cos\alpha = \frac{B}{\hat{a}} + \cos\theta \quad (43)$$

In equations(41)-(43) $\pi > \theta > 0$, and $B > \hat{a} > \frac{B}{2}$. The function (41) is such that

$$t_{xy}(\theta + \pi) = -t_{xy}(\theta) \quad (44)$$

For larger values of $\hat{a}$ the expressions are simplified. From Fig. 13c we see that all junctions except those formed less than a half-cycle ago have been destroyed in this case. Thus for $0 < \theta < \xi$,

$$\frac{t_{xy}}{\omega\,\hat{a}} = \cos\theta \sum_n \frac{a_n}{\Lambda_n}\left[1 - \exp -(\theta+\xi)/\Lambda_n\right] - \sum_n \frac{a_n}{1+\Lambda_n^2}\left[\frac{\cos\theta}{\Lambda_n} + \sin\theta\right]$$

$$+ \sum_n a_n \frac{\exp -(\theta+\xi)/\Lambda_n}{1+\Lambda_n^2}\left[\frac{\cos\xi}{\Lambda_n} - \sin\xi\right] \qquad (45)$$

For $\xi \leq \theta < \delta$, where

$$\cos\delta = 1 - 2B/\hat{a} \qquad (46)$$

we have

$$\frac{t_{xy}}{\omega\hat{a}} = \text{Expression (45)} - \frac{t_{xy}^{(1)}}{\omega\hat{a}} \qquad (47)$$

where

$$\frac{t_{xy}^{(1)}}{\omega\hat{a}} = 2\cos\theta \sum_n \frac{a_n}{\Lambda_n} \exp - \theta/\Lambda_n \sinh\left(\frac{\alpha}{\Lambda_n}\right)$$

$$- 2\sum_n \frac{a_n \exp - \theta/\Lambda_n \cos\alpha}{\Lambda_n(1+\Lambda_n^2)} \sinh\left(\frac{\alpha}{\Lambda_n}\right)$$

$$- 2\sum_n \frac{a_n \exp - \theta/\Lambda_n}{1+\Lambda_n^2} \sin\alpha \cosh\left(\frac{\alpha}{\Lambda_n}\right) \qquad (48)$$

while for $\pi > \theta > \delta$ we have

$$\frac{t_{xy}}{\omega\,\hat{a}} = \cos\theta \sum_n \frac{a_n}{\Lambda_n}(1 - \exp - (\theta - \delta)/\Lambda_n)$$

$$- \sum_n \frac{a_n}{1+\Lambda_n^2}\left[\frac{\cos\theta}{\Lambda_n} + \sin\theta\right]$$

$$+ \sum_n \frac{a_n \exp -(\theta-\delta)/\Lambda_n}{1+\Lambda_n^2}\left[\frac{\cos\delta}{\Lambda_n} + \sin\delta\right] \qquad (49)$$

Some of these expressions are portrayed in figs. 15 and 16 for the fluids shown in fig. 14. In both cases $\eta_o = 1$ poise and there is a single time constant. For fluid A $\eta_\infty = 0.6$ poise and for fluid B $\eta_\infty = 0$. In both cases we choose $\hat{a} = 4$, $B = 2$, $A = 1$. Fig. 15 shows the response for fluid A and for the same fluid with $B > 8$ (linear viscoelasticity). The flattening of the curve in the region of maximum speed and the reduced elasticity as evinced by the very much reduced phase shift (measured by the curve intercepts on the θ-axis) show clearly. The third harmonic appears to be about 6% of the fundamental. Philippoff,[26] experimenting with a fluid having properties similar toA, gives the same general predictions and the same size of third harmonic (< 10%). Fluid B shows a more dramatic change from the linear case, fig. 16. The third harmonic is about 30% greater than the first in this case and again the phase shift is reduced. A curve is drawn on fig. 16 indicating a linear response cut down by assuming η_o to be that corresponding to the mean shear rate γ_m, where

$$\gamma_m = 2\hat{a}\omega/\pi \qquad (50)$$

This fails to predict phase, amplitude or harmonic content changes.

The rupture theory has not been compared with the Bird-Macdonald[10] model here. The latter gives rise to integrals not expressible in terms of tabulated functions.

5. Elongational Flows

We have seen that the two simple integral models discussed above behave similarly in shearing flows. Although a great many laminar flows of interest belong to this category it is desirable to test any new constitutive approximations in other types of flow. Recently the simple

extensional flows have become of some interest[4,33] and here we consider two-dimensional (sheet) and three-dimensional (rod) extensions.

For the sheet case (pure shear) the velocity field is of the form

$$\underline{V} = (Gx, -Gy, 0) \tag{51}$$

and the rate of deformation matrix has diagonal elements G, -G, 0 respectively. From reference 4 we find the strain field $\underline{\underline{B}}(t')$ also has a diagonal form with non-zero elements as follows

$$\begin{aligned} B_{xx} &= e^{2G(t-t')} - 1 \\ B_{yy} &= e^{-2G(t-t')} - 1 \end{aligned} \tag{52}$$

Computing $t_{xx}-t_{yy}$ by assuming $t_{yy} = 0$ (ambient pressure) we find

$$t_{xx}-t_{yy} = \int_{t-\tau_R}^{t} 2N\,(t-t')\sinh 2G\,(t-t')\,dt' \tag{53}$$

and also

$$\operatorname{tr} \underline{\underline{B}}(t') = 2[\cosh 2G\,(t-t') - 1] = B^2 \tag{54}$$

Equation (54) defines the rupture time τ_R as

$$\tau_R = \frac{1}{2G}\cosh^{-1}\left(1 + \frac{B^2}{2}\right) \tag{55}$$

Integrating, we find, for n discrete relaxation times,

$$t_{xx} - t_{yy} = \sum^{n} \frac{a_n}{\lambda_n}\left[\frac{\exp \tau_R(2G-1/\lambda_n) - 1}{2G\lambda_n - 1} + \frac{\exp -\tau_R(2G+1/\lambda_n) - 1}{2G\lambda_n + 1}\right] \tag{56}$$

The corresponding result for the Bird-Macdonald model is, for $1 > 2G\lambda_n$,

$$t_{xx} - t_{yy} = \sum^{n} \frac{4a_n}{\lambda_n(1+2c^2\lambda_n^2G^2)(1-4G^2\lambda_n^2)} \tag{57}$$

For $2G\lambda_n > 1$ the integrals leading to (57) diverge and no solution is at hand. The results (56) and (57) are compared in Fig. 17 for $B = 3$, $c = 1.68/B$; here

$$\eta_{e_2} = (t_{xx}-t_{yy})/G \tag{58}$$

The results for a three-dimensional (rod) elongation have been given previously[2]. Fig. 18 shows the results for a single time constant with various values of breaking strain $\bar{B}$. The quantity $\bar{B}$ is related to B (in pure shear) by the equation

$$\bar{B} = \frac{1}{2}\cosh^{-1}\left(1 + \frac{B^2}{2}\right) \equiv \tau_R G \tag{59}$$

with a similar result for simple extension[2]. With these results it is possible to make an attempt at explaining the results of Ballman[33] using the rupture theory. Since no dynamic measurements are available only two time constants have been used. We take $\lambda_1 = 200$ sec , $\lambda_2 = 20$ sec , with $a_1 = 467$ lbf.s/in^2, $a_2 = 200$ lbf.s/in.^{2} These values correspond to the extrapolated (dashed) curves in fig. 19, which are not impossible. With $\bar{B} = 2.5$ $(B = 12.2)$ we find a hump in the elongational viscosity of the right order of magnitude. Further terms in the kernel would improve the shape of the hump if required. It is discussed elsewhere[13] that solid materials will be expected to have larger values of B than solutions. Accepting this, then the mystery of high, but not infinite, elongational viscosities disappears.

Discussion

This paper has attempted a comparative study of the network rupture theory and other simple integral theories. Both of the principal theories considered need only the following tests for estimation of the

parameters involved:

(a) The dynamic viscosity. This fixes the form of $N(\tau)$ and allows the a_n , λ_n to be chosen.

(b) The shear-stress-shear-rate curve. Using this data with test (a) one can find the rupture strain magnitude (B). In the Bird-Macdonald theory[10] c may be found in a similar way.

(c) The second normal stress difference allows ϵ to be estimated.

Providing one is willing to accept the type of spectrum used by Spriggs et al[4] one could say that both theories require five constants. This aspect has not been emphasized here. The first normal stress difference and the rest of the uniform stress tests given above are predicted with no further parameter adjustment. If one was willing to pick the best overall value of B (or c) to fit both viscosity and normal stress data quite close agreement with these tests could be obtained. Then, however, one cannot strictly say that the first normal stress is predicted. Doughty and Bogue[27] have effectively tried this approach; some of their results for the BKZ[28] model are identical to the Bird-Macdonald model (eqn. 12) while Bogue's own model[8] yields the type of result given in equation (8). According to this work[27], the Bogue and BKZ models are more accurate than Pao's[29] model or a differential model of the Oldroyd type[30]. In the present writer's opinion the Bogue and BKZ models are not superior in convenience, accuracy or physical insight to the Bird-Macdonald[10] model in simple shearing. For more complex flows they are decidedly more inconvenient. Furthermore, all of these theories predict infinite stresses in pure shearing at a finite shearing rate. The present author considers that this is an unrealistic prediction, but this is not a universally held opinion[31,32].

Evidence supporting this idea occurs in the data of Ballman[33] and Nitschmann[34] whose data show that some of the relaxation times are greater than $1/2\ G$. Astarita[32] has stated that "fluids for which the rate of stress relaxation is essentially exponential may flow at any value of $\lambda\sqrt{II_d}$ without developing infinite stresses, but cannot flow at values of $\lambda\sqrt{II_d - II_\omega}$ exceeding some critical upper limit of the order of unity". Here II_ω is the second invariant of the vorticity tensor. Referring to equations (32) and fig. 18 we immediately see that Astarita's[32] conclusion is false. Our rupture theory relaxes exponentially and does not have a maximum shear rate. The network theory of Yamamoto[35] also shows no maximum shear rate. One suspects that a proper three-dimensional formulation of the work of Graessley[36] would show a maximum shear rate effect. Thus it is concluded that network rupture, which is a natural physical effect, is effective in suppressing these unrealistic infinite stresses at finite elongation rates.

It would also be possible to use something like the rate factor $[1 + 2c^2\lambda^2 II(t')]^{-1}$ to represent the effect of shearing on junction formation while retaining the network rupture for terminating old junctions. Such a composite theory seems to be physically reasonable and would allow a better fit (not prediction) of the first normal stress difference at higher shear rates. In many cases the extra complexity would not be warranted, one suspects, and the simple rupture theory will be adequate.

The deficiencies of the present model appear to be associated with most simple isotropic fluids and it is hard to see how much improvement in fitting the combined shear test (fig. 7) for example, can be made without tremendous computational disabilities[19]. Probably the best approach now lies in the study of the molecular constitution rather than in

pure continuum mechanics. Obviously details of the network formation and rupture should be considered and some improvements can certainly be made in this direction. Scope also clearly exists for further critical experimental work in testing the various theories on different fluids and developing computational methods for more complex flows. The author is not convinced that a perfect fit to all existing data will ever be made with simple integral models of the type considered here. However, it is encouraging that opinion is now converging on this type of theory as representing the best type of simple constitutive equation for polymer fluids.

Acknowledgements

I am grateful to Dr. J. M. Simmons for permission to use experimental data from his Ph.D. thesis in some of the comparisons. The preparation of this paper and the conduct of some of the experiments were supported by the National Aeronautics and Space Administration under the Multidisciplinary Space-Related Research Program (Grant NGL-40-002-009) at Brown University. This support is gratefully acknowledged.

References

1. Spriggs, T. W., J. D. Huppler and R. B. Bird. Trans. Soc. Rheol. 10:1, 191-213 (1966).

2. Tanner. R. I. and J. M. Simmons. Chem. Eng. Sci. 22, 1079-1082 (1967).

3. Tanner, R. I. and J. M. Simmons. Chem. Eng. Sci., 22 (to appear).

4. Lodge, A. S. Elastic Liquids, Academic Press, New York, 1964.

5. Finger, J. Sitzgsber. Akad. Wiss. Wien (IIa) 103, 163-200 (1894) (also pp. 231-250).

6. Green, G. Trans. Cambr. Phil. Soc., 7, 121-140 (1841).

7. Bogue, D. C. and J. O. Doughty. I. & E. C. Fund. 5, 243-252 (1966).

8. Bogue, D. C. I. & E. C. Fundamentals 5, 253-259 (1966).

9. Ferry, J. D. Viscoelastic Properties of Polymers, Wiley, New York, 1961.

10. Macdonald, I. F. and R. B. Bird. J. Phys. Chem. 70, 2068-2069 (1966).

11. Rouse, P. E. J. Chem. Phys. 21, 1272-1280 (1963).

12. Kaye, A. Brit. J. Appl. Phys. 17, 803-806 (1966).

13. Tanner, R. I. To appear. "Molecular Aspects of a Network Rupture Theory."

14. Coleman, B. D., H. Markovitz and W. Woll. Viscometric Flows of non-Newtonian Fluids, Springer-Verlag, Berlin, 1966.

15. Markovitz, H. and B. D. Coleman. Adv. in Applied Mech. 8, 69-101 (1964).

16. Philippoff, W. Trans. Rheol. Soc. 10:1, 1-24 (1966).

17. Huppler, J. D. Trans. Soc. Rheol. 9:2, 273-286 (1965).

18. Bird, R. B. Unpublished note (1966), "Oscillatory shear with superposed transverse steady shear."

19. Simmons, J. M. Ph.D. thesis, University of Sydney, 1967.

20. Simmons, J. M. J. Sci. Instr. 43, 887-892 (1966).

21. Osaki, K., M. Tamura, M. Kurata and T. Kotaka. J. Soc. Mat. Sci. Japan, 12, 339-340 (1963).

22. Osaki, K., M. Tamura, M. Kurata and T. Kotaka. J. Phys. Chem. 69, 4183-4191 (1965).

23. Booij, H. C. Rheol. Acta, 5, 215-221 (1966).

24. Booij, H. C. Rheol. Acta, 5, 222-227 (1966).

25. Billington, E. W. and A. S. Huxley. Trans. Faraday Soc. 61, 2784-2793 (1965).

26. Philippoff, W. Trans. Soc. Rheol. 10:1, 317-334 (1966).

27. Doughty, J. O. and D. C. Bogue. I. & E. C. Fundls. 6, 388-393 (1967).

28. Bernstein, B., E. Kearsley and L. Zapas. Trans. Soc. Rheol. 7, 391-410 (1963).

29. Pao, Y. H. J. Appl. Phys. 28, 591-598 (1957).

30. Williams, M. C. and R. B. Bird. Phys. Fluids 5, 1126-1127 (1962).

31. Seyer, F. A. and A. B. Metzner. Can. J. Chem. Eng. 45, 121-126 (1967).

32. Astarita, G. I. & E. C. Fundls. 6, 257-262 (1967).

33. Ballman, R. L. Rheol. Acta 4, 137-140 (1965).

34. Nitschmann, H. Proc. Ist. Intl. Congr. Rheol., North-Holland, Amsterdam, 1949, pp. II-32-34.

35. Yamamoto, M. J. Phys. Soc. Japan 12, 1148-1158 (1957).

36. Graessley, W. W. J. Chem. Phys. 43, 2696-2703 (1965).

Captions for Figures

Fig. 1. Comparison of theoretical viscosity and normal stress curves.

Fig. 2. Comparison with viscosity data for 5.4% polyisobutylene-cetane solution at 25°C.

Fig. 3. Comparison of normal stress data and dynamic elasticity.

Fig. 4. Experimentally observed ratio of normal stress differences.

Fig. 5. Response to combined sinusoidal and simple shearing (transverse case) for a single time constant. Viscosity data.

Fig. 6. Combined shear test (transverse case). Elasticity data.

Fig. 7. Comparison of combined shearing with experiments on a 5.4% p.i.b/cetane solution. Viscosity data.

Fig. 8. Comparison of combined shearing with experiments on 5.4% p.i.b/cetane solution. Elasticity data.

Fig. 9. Experimental data for 1.5% carboxymethylcellulose-water solution. Viscosity data.

Fig. 10. CMC-water solution. Elasticity data.

Fig. 11. Combined sinusoidal and simple shearing (parallel case) for a single time constant. Elasticity data.

Fig. 12. Start-shear theoretical curves.

Fig. 13. Regions of network rupture in finite amplitude sinusoidal shearing.

Fig. 14. Theoretical viscosity functions A and B.

Fig. 15. Response to finite amplitude sinusoidal shearing. Fluid A.

Fig. 16. Response to finite amplitude sinusoidal shearing. Fluid B.

Fig. 17. Pure shear results for a single time constant.

Fig. 18. Elongational flow results for rupture theory.

Fig. 19. Comparison of rupture theory and experiment of Ballman[33].

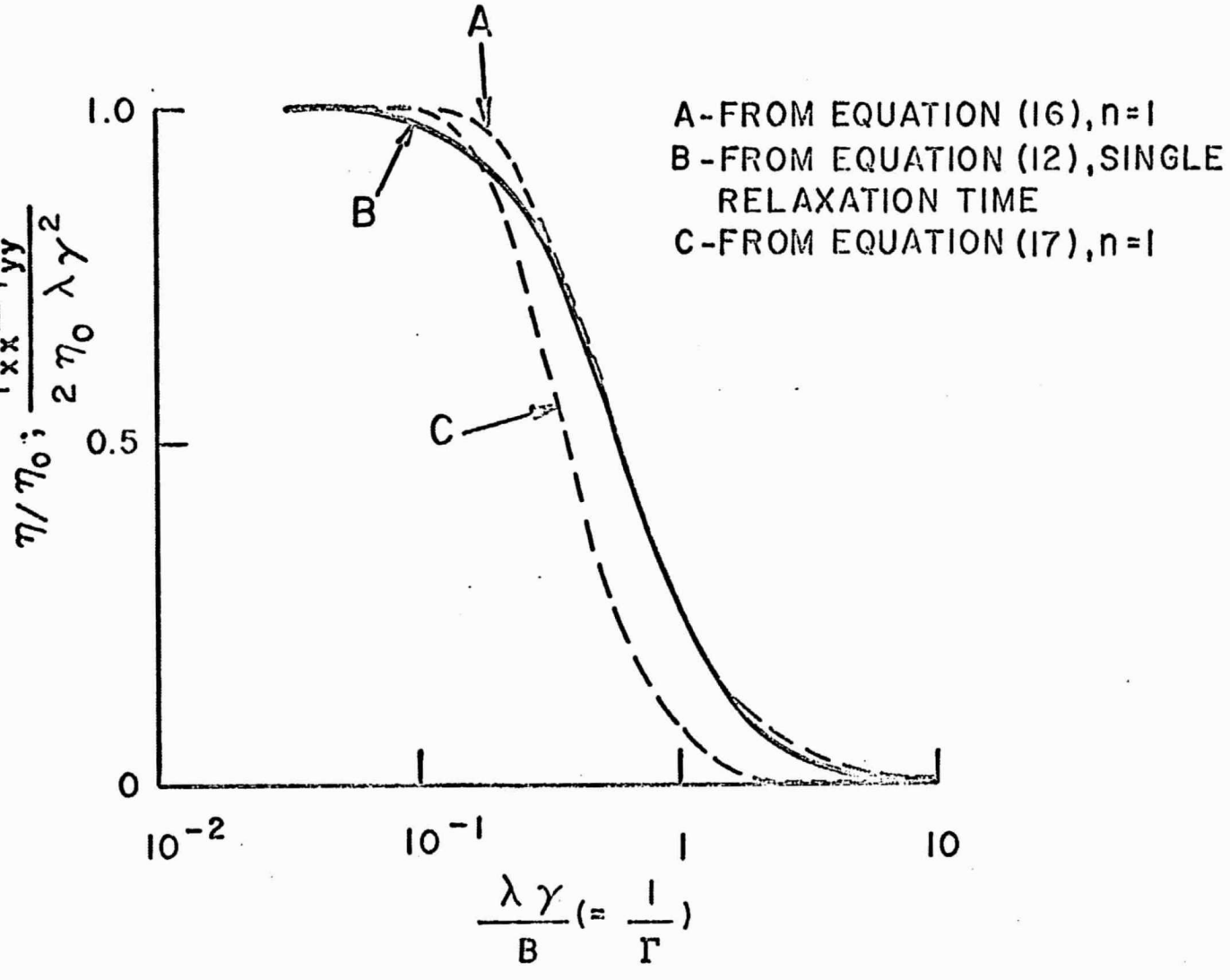
A
B
C
1.0
0.5
0
10^{-2}
10^{-1}
1
10
$\eta/\eta_0 ; \frac{t_{xx}-t_{yy}}{2\eta_0 \lambda \gamma^2}$
$\frac{\lambda\gamma}{B} (= \frac{1}{\Gamma})$
A-FROM EQUATION (16), n=1
B-FROM EQUATION (12), SINGLE RELAXATION TIME
C-FROM EQUATION (17), n=1

FIG. 1

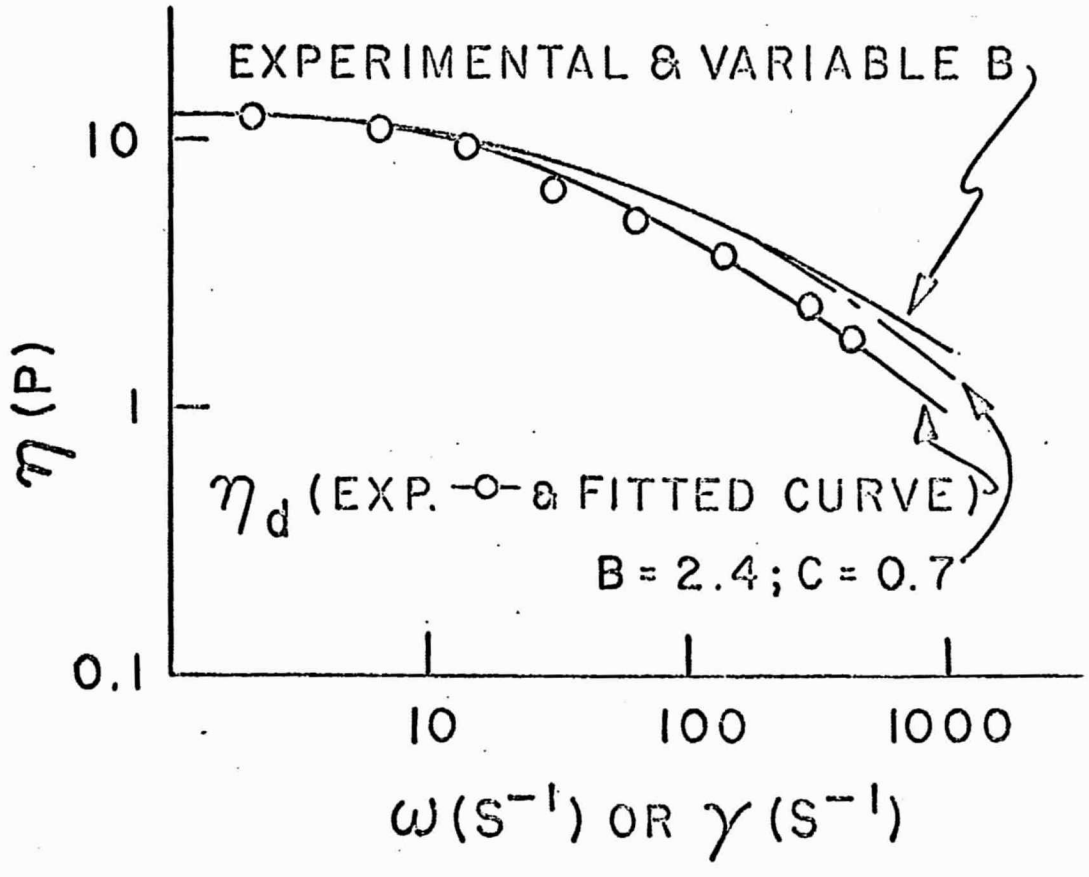
EXPERIMENTAL & VARIABLE B
10
1
0.1
η (P)
η_d (EXP. —o— & FITTED CURVE)
B = 2.4 ; C = 0.7
10
100
1000
ω (S⁻¹) OR γ (S⁻¹)

FIG. 2

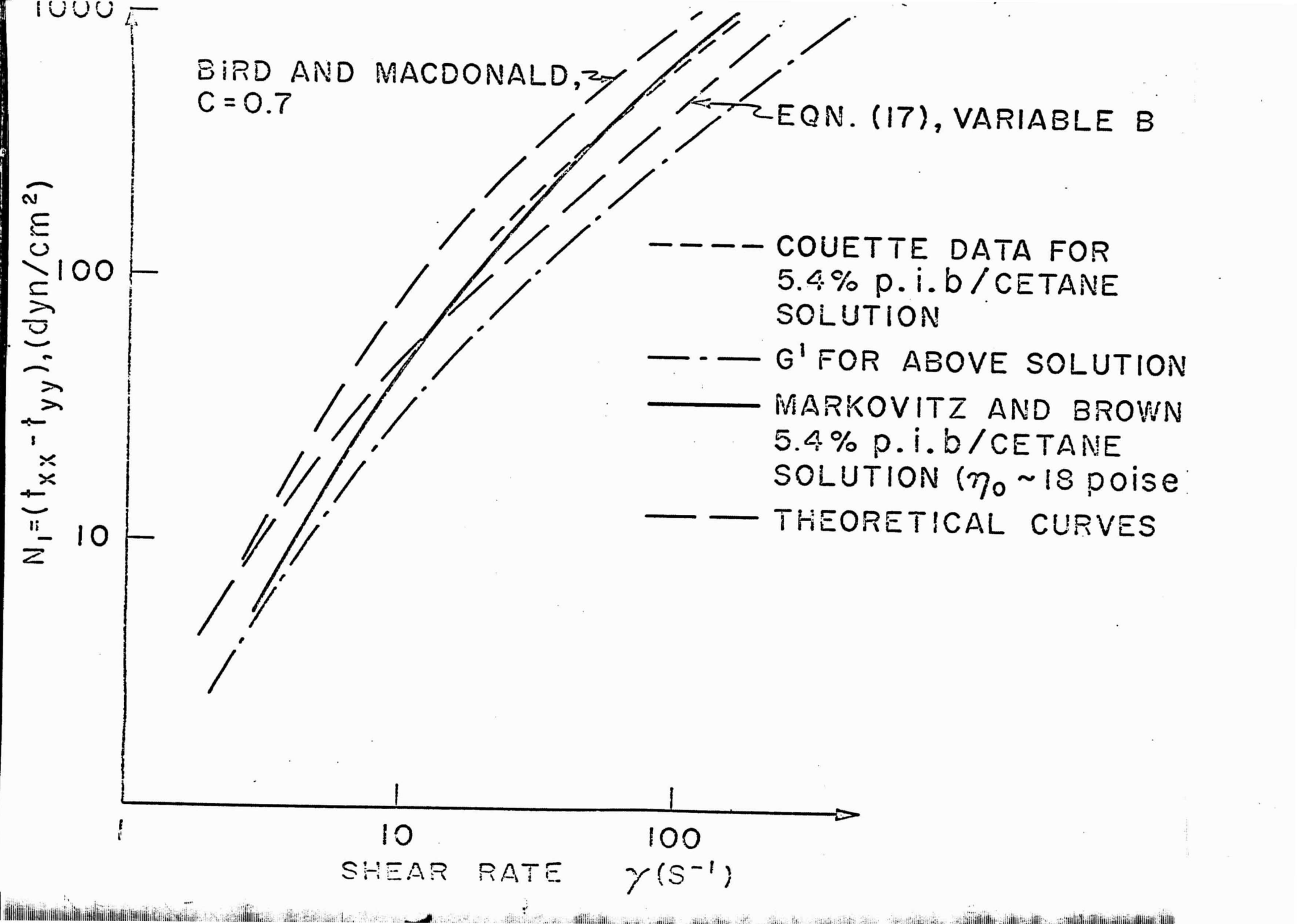
1000
100
10
1
$N_1=(t_{xx}-t_{yy})$, (dyn/cm²)
BIRD AND MACDONALD, C=0.7
EQN. (17), VARIABLE B
COUETTE DATA FOR 5.4% p.i.b/CETANE SOLUTION
G' FOR ABOVE SOLUTION
MARKOVITZ AND BROWN 5.4% p.i.b/CETANE SOLUTION (η_0 ~ 18 poise
THEORETICAL CURVES
1
10
100
SHEAR RATE $\gamma(S^{-1})$

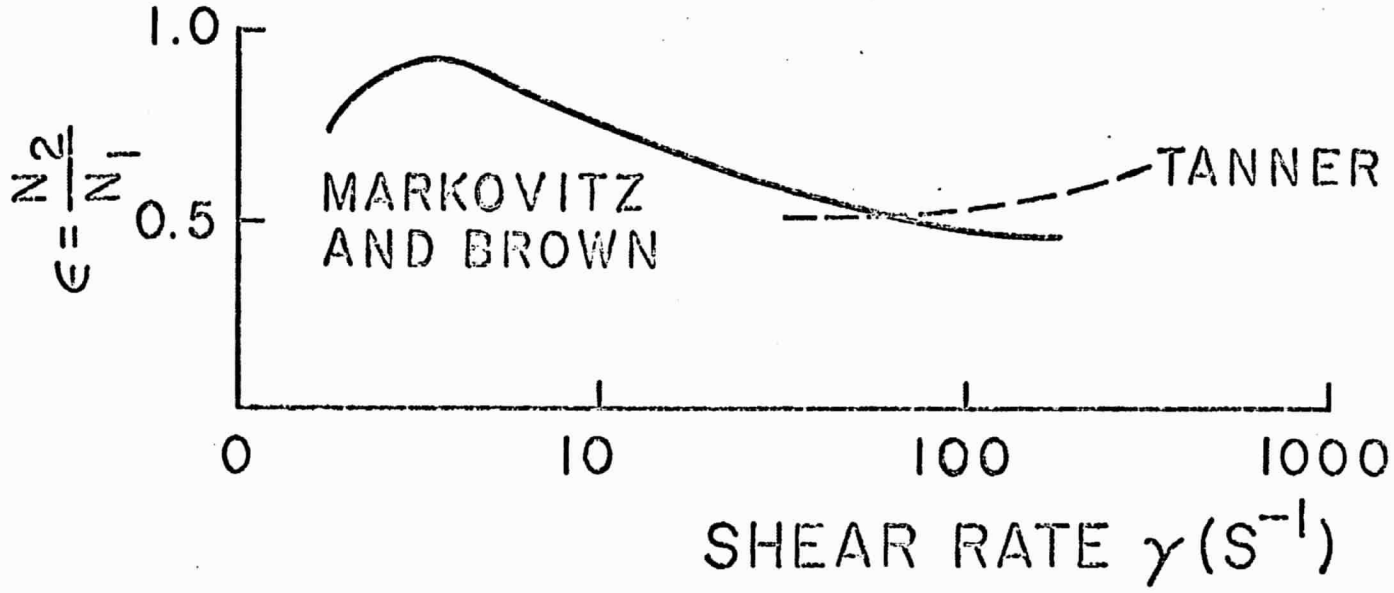
1.0
0.5
$\Psi = N_2/N_1$
MARKOVITZ
AND BROWN
TANNER
0
10
100
1000
SHEAR RATE $\gamma (S^{-1})$

FIG. 4

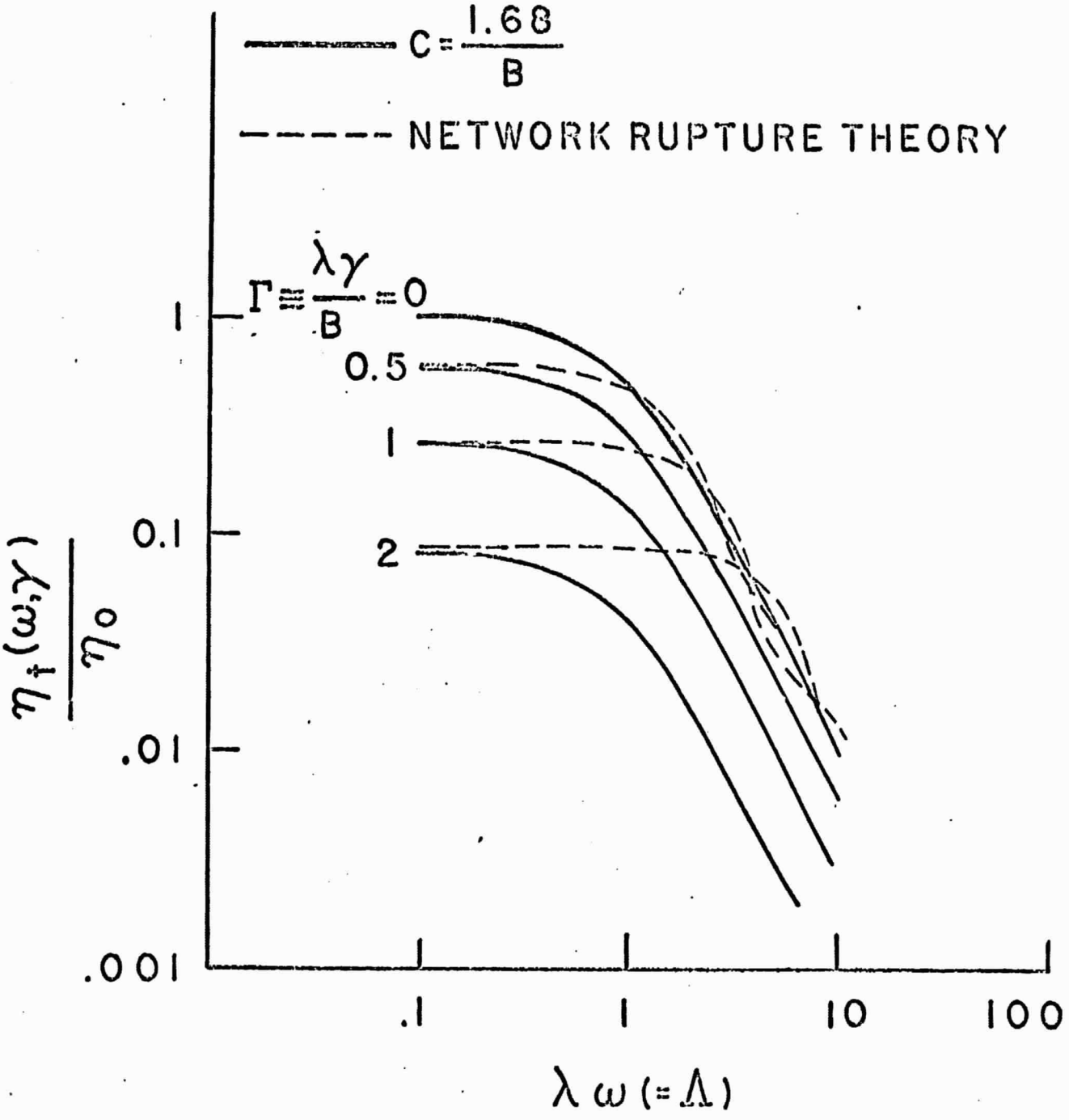
C = 1.68/B
NETWORK RUPTURE THEORY
Γ ≡ λγ/B = 0
0.5
1
2
η+(ω,γ)/η0
1
0.1
.01
.001
.1
1
10
100
λω (= Λ)

FIG. 5.

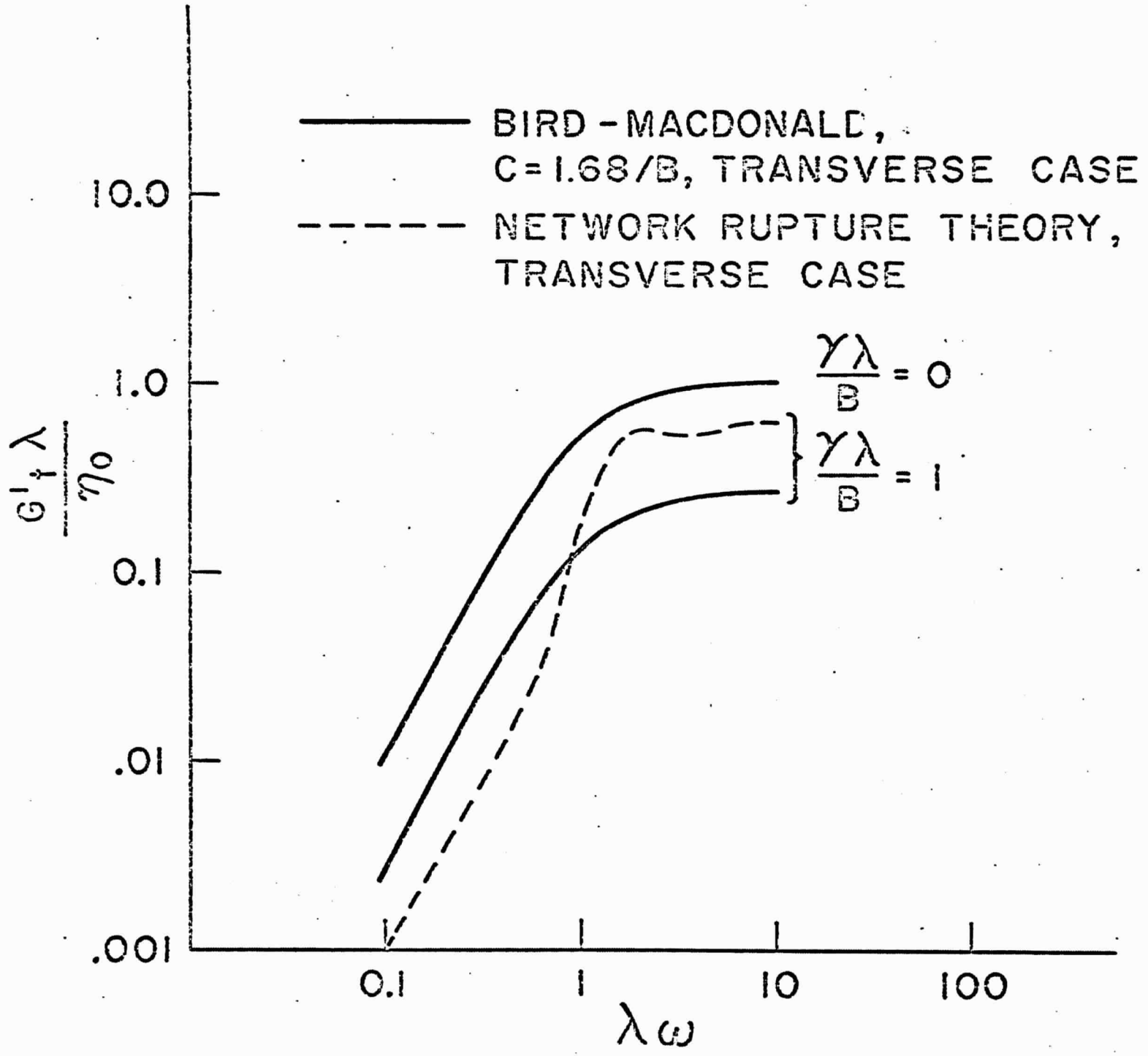
BIRD - MACDONALD,
C = 1.68/B, TRANSVERSE CASE
NETWORK RUPTURE THEORY,
TRANSVERSE CASE
$\frac{\gamma\lambda}{B} = 0$
$\frac{\gamma\lambda}{B} = 1$
$\frac{G'_t \lambda}{\eta_0}$
10.0
1.0
0.1
.01
.001
0.1
1
10
100
$\lambda\omega$

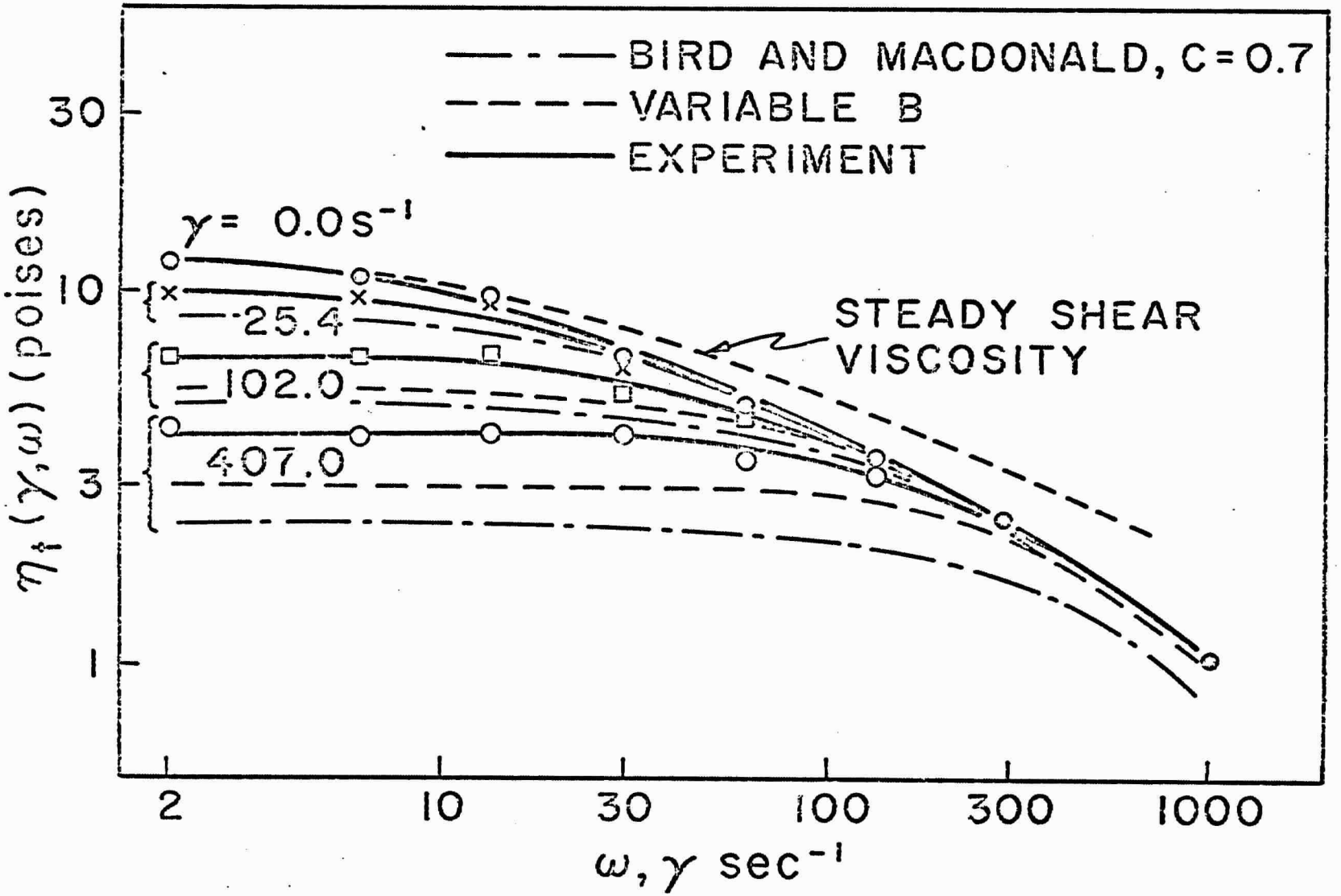
BIRD AND MACDONALD, C = 0.7
VARIABLE B
EXPERIMENT
γ = 0.0 s^{-1}
25.4
102.0
407.0
STEADY SHEAR VISCOSITY
$\eta_+(\gamma,\omega)$ (poises)
30
10
3
1
2
10
30
100
300
1000
ω, γ sec^{-1}

Fig. 7

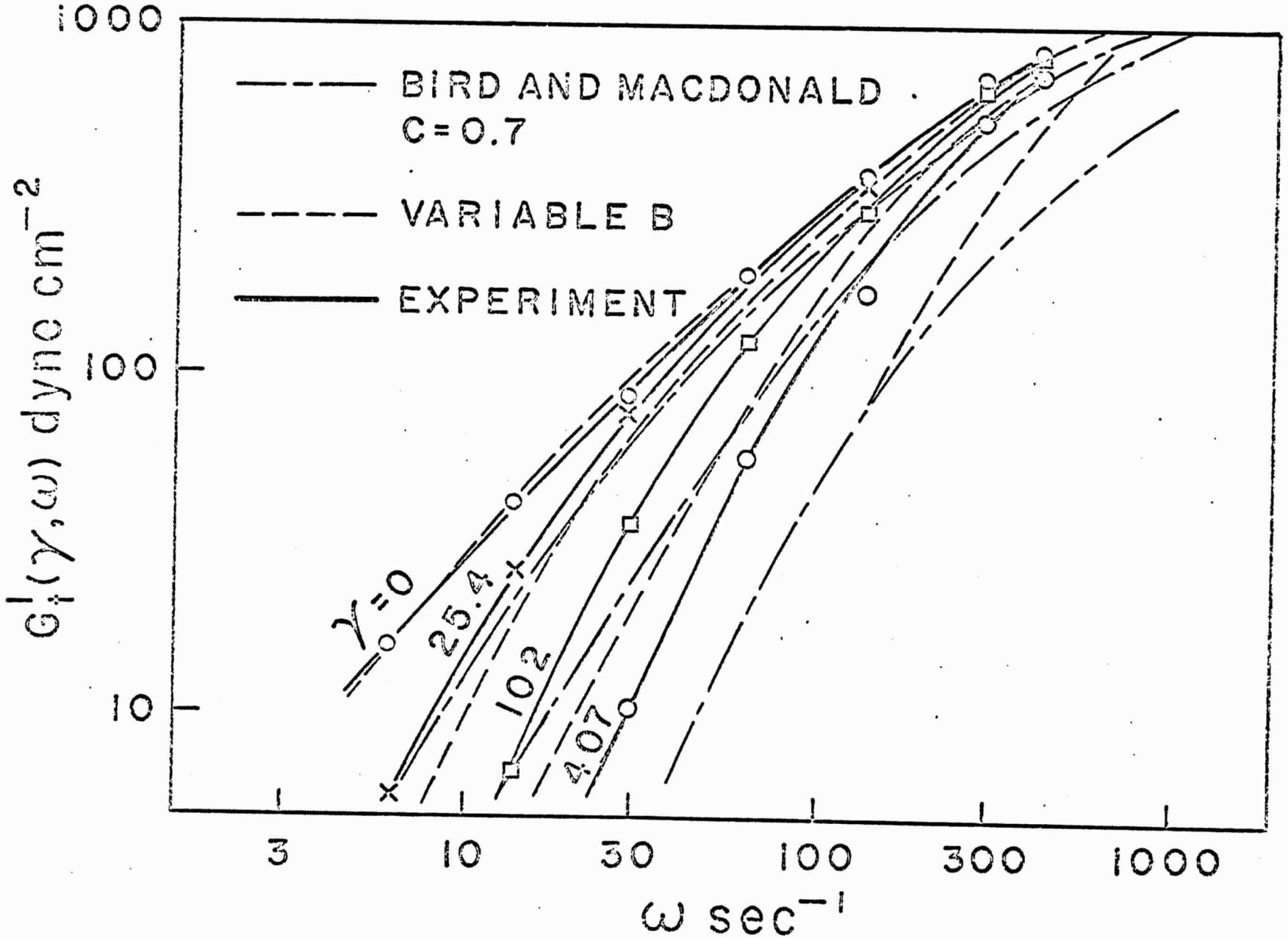
1000
100
10
$G_+^1(\gamma,\omega)$ dyne cm^{-2}
BIRD AND MACDONALD
C = 0.7
VARIABLE B
EXPERIMENT
γ=0
25.4
102
407
3
10
30
100
300
1000
ω sec^{-1}

FIG. 2

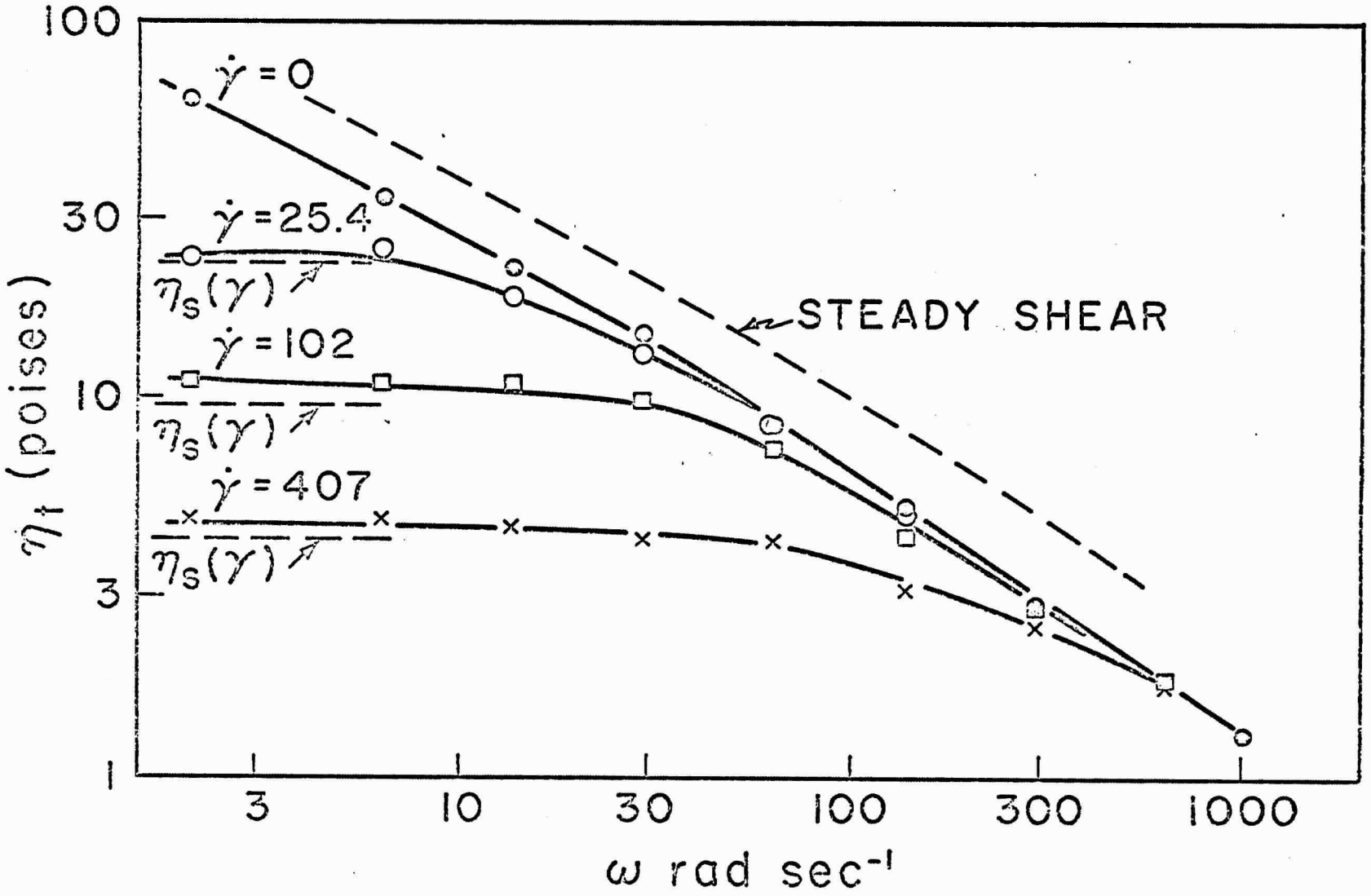
100
30
10
3
1
η_t (poises)
$\dot{\gamma} = 0$
$\dot{\gamma} = 25.4$
$\eta_s(\gamma)$
$\dot{\gamma} = 102$
$\eta_s(\gamma)$
$\dot{\gamma} = 407$
$\eta_s(\gamma)$
STEADY SHEAR
3
10
30
100
300
1000
ω rad sec^{-1}

FIG. 7.

ELASTIC MODULUS G' dynes-cm⁻²
0
10^2
10^3
10
100
1000
ω rad sec-1
γ=0
γ=25.4 sec-1
γ=102 sec-1
γ=407sec-1

Fig. 10

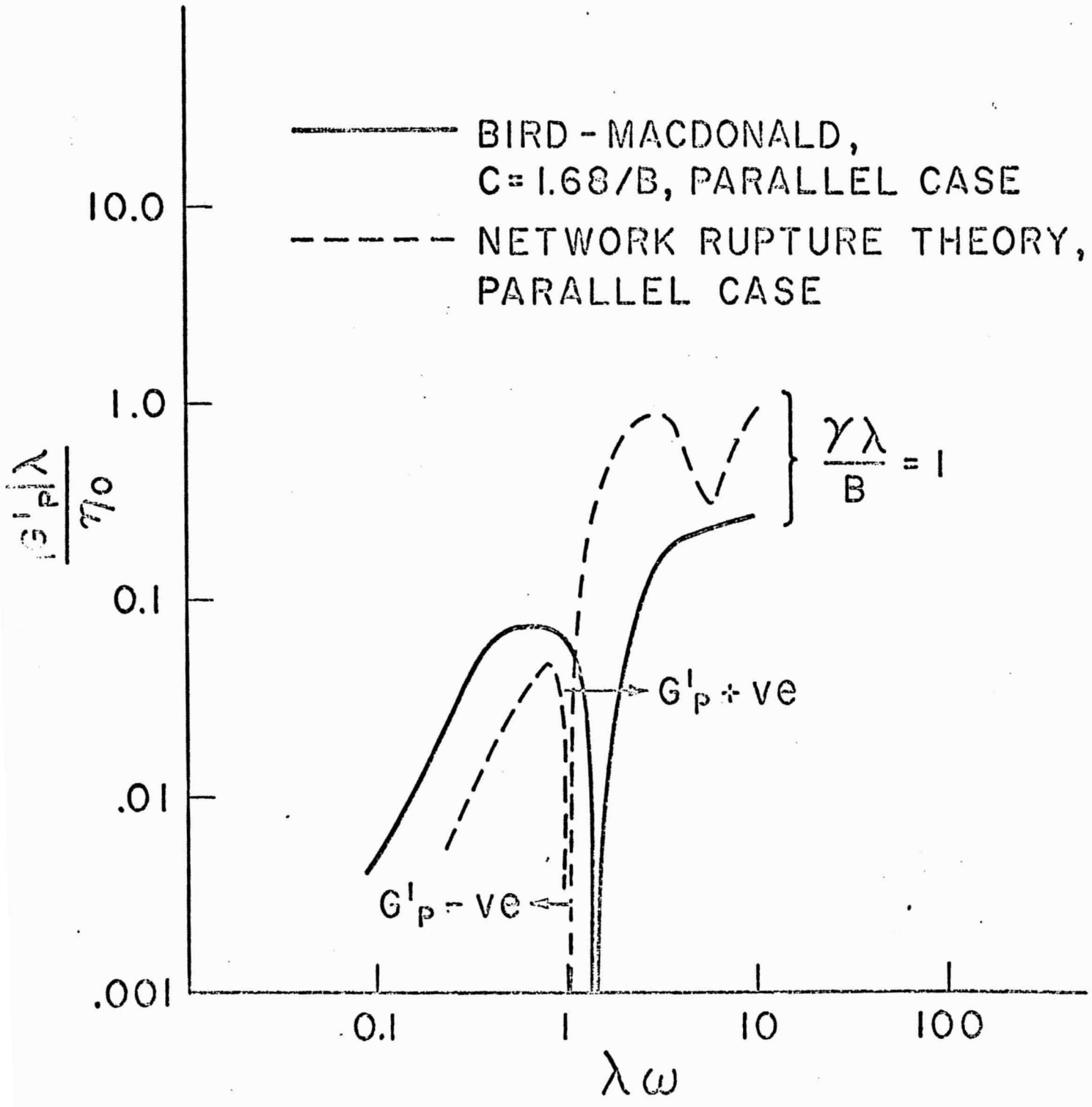
BIRD - MACDONALD,
C = 1.68/B, PARALLEL CASE
NETWORK RUPTURE THEORY,
PARALLEL CASE
10.0
1.0
0.1
.01
.001
$\frac{|G'_{pl}|\lambda}{\eta_0}$
$\frac{\gamma\lambda}{B} = 1$
G'_p + ve
G'_p - ve
0.1
1
10
100
$\lambda\omega$

FIG

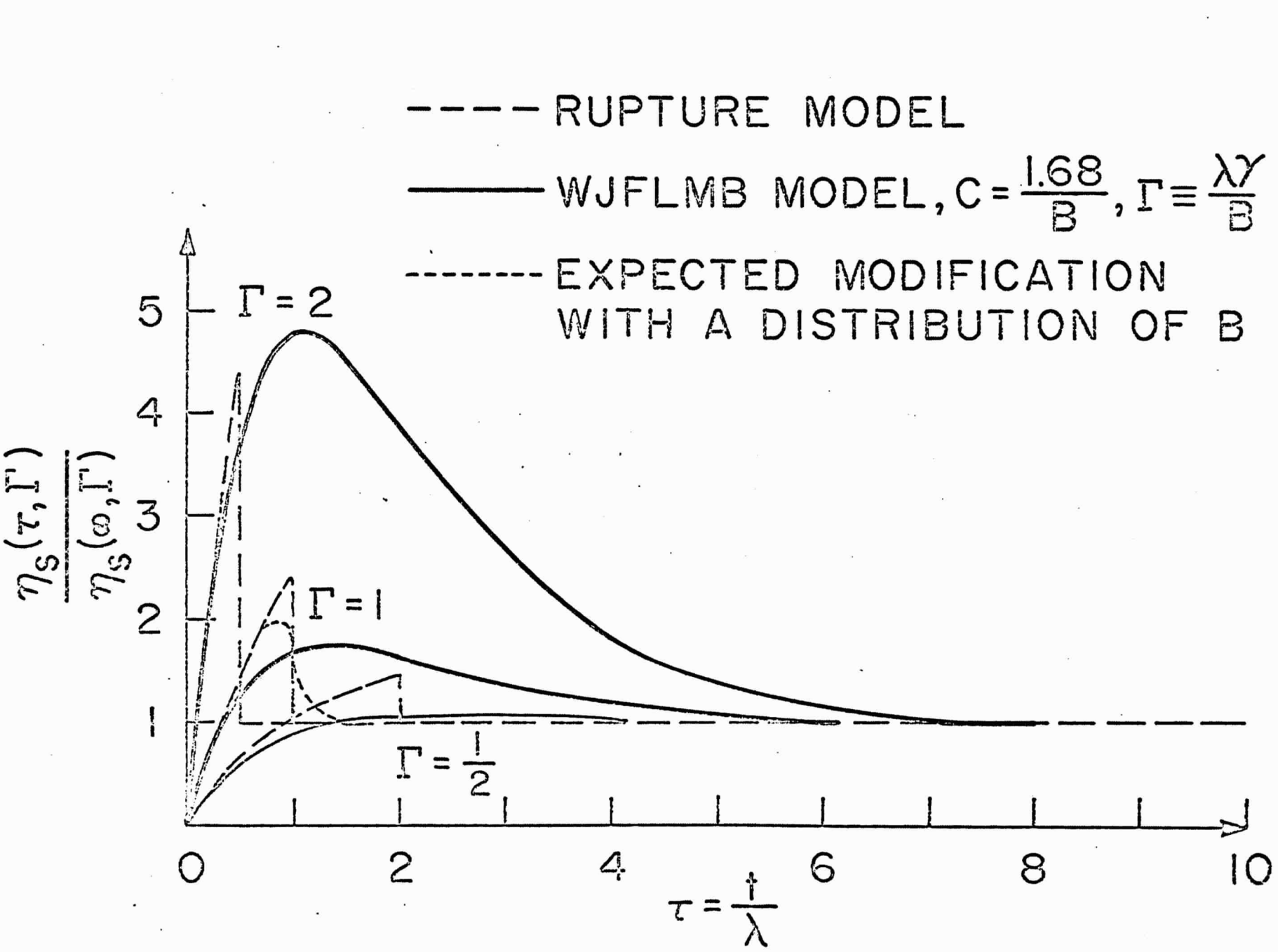
RUPTURE MODEL
WJFLMB MODEL, $C = \frac{1.68}{B}$, $\Gamma \equiv \frac{\lambda\gamma}{B}$
EXPECTED MODIFICATION WITH A DISTRIBUTION OF B
$\frac{\eta_s(\tau,\Gamma)}{\eta_s(\infty,\Gamma)}$
$\Gamma = 2$
$\Gamma = 1$
$\Gamma = \frac{1}{2}$
$\tau = \frac{t}{\lambda}$
0
2
4
6
8
10
1
2
3
4
5

FIG. 12

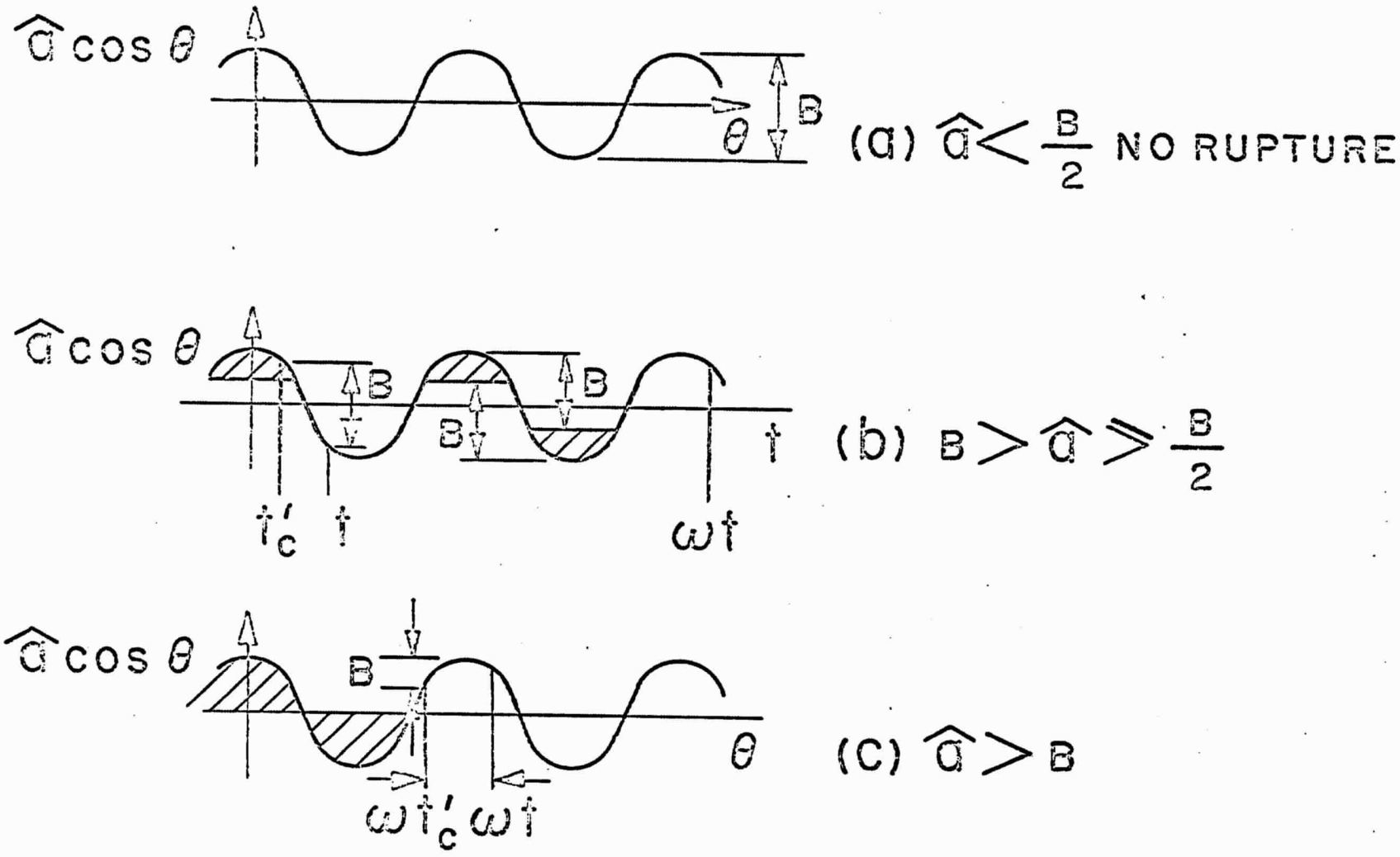
$\hat{a}\cos\theta$
B
θ
(a) $\hat{a} < \frac{B}{2}$ NO RUPTURE
$\hat{a}\cos\theta$
B
B
B
t
t_c' t
ωt
(b) $B > \hat{a} \geqslant \frac{B}{2}$
$\hat{a}\cos\theta$
B
θ
$\omega t_c'$ ωt
(C) $\hat{a} > B$
/// DENOTES RUPTURE REGIONS

FIG. 13

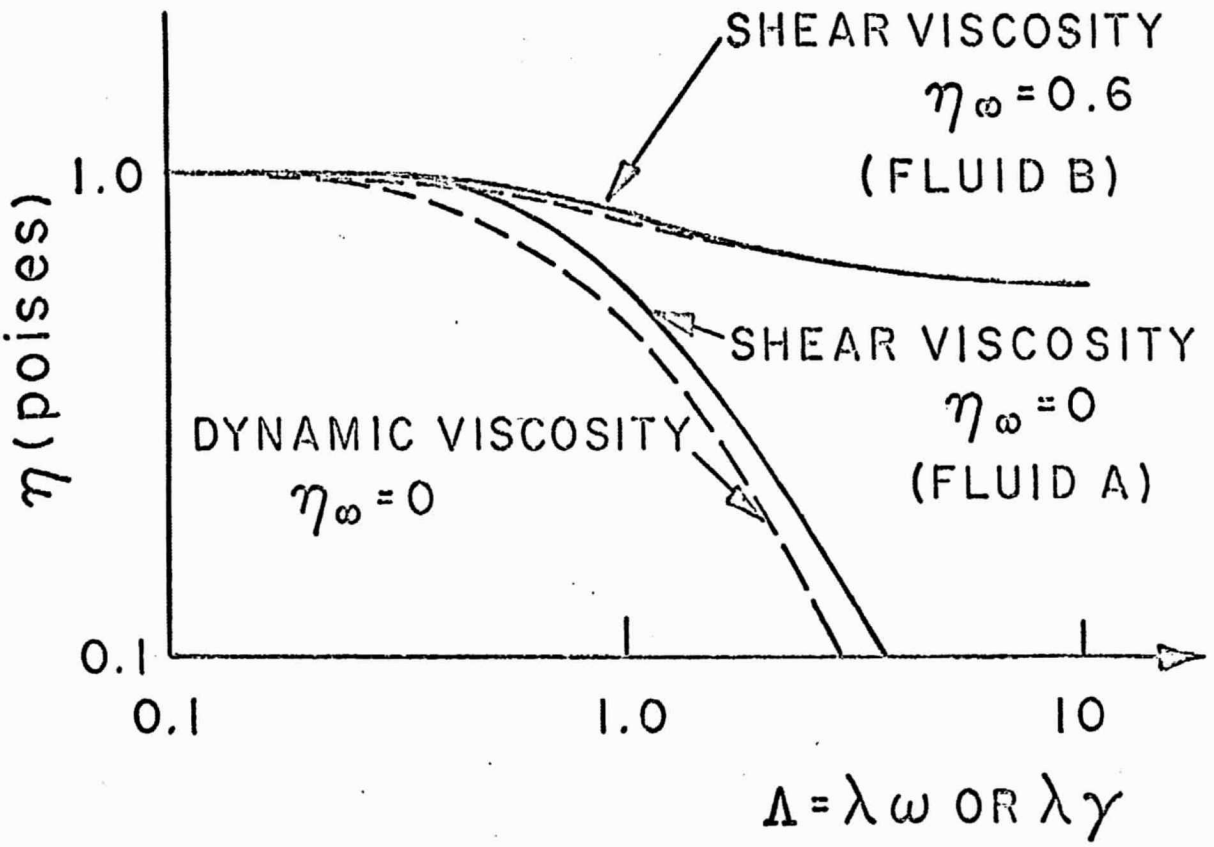
SHEAR VISCOSITY
$\eta_\infty = 0.6$
(FLUID B)
SHEAR VISCOSITY
$\eta_\infty = 0$
(FLUID A)
DYNAMIC VISCOSITY
$\eta_\infty = 0$
η (poises)
1.0
0.1
0.1
1.0
10
$\Lambda = \lambda\omega$ OR $\lambda\gamma$

FIG. 14

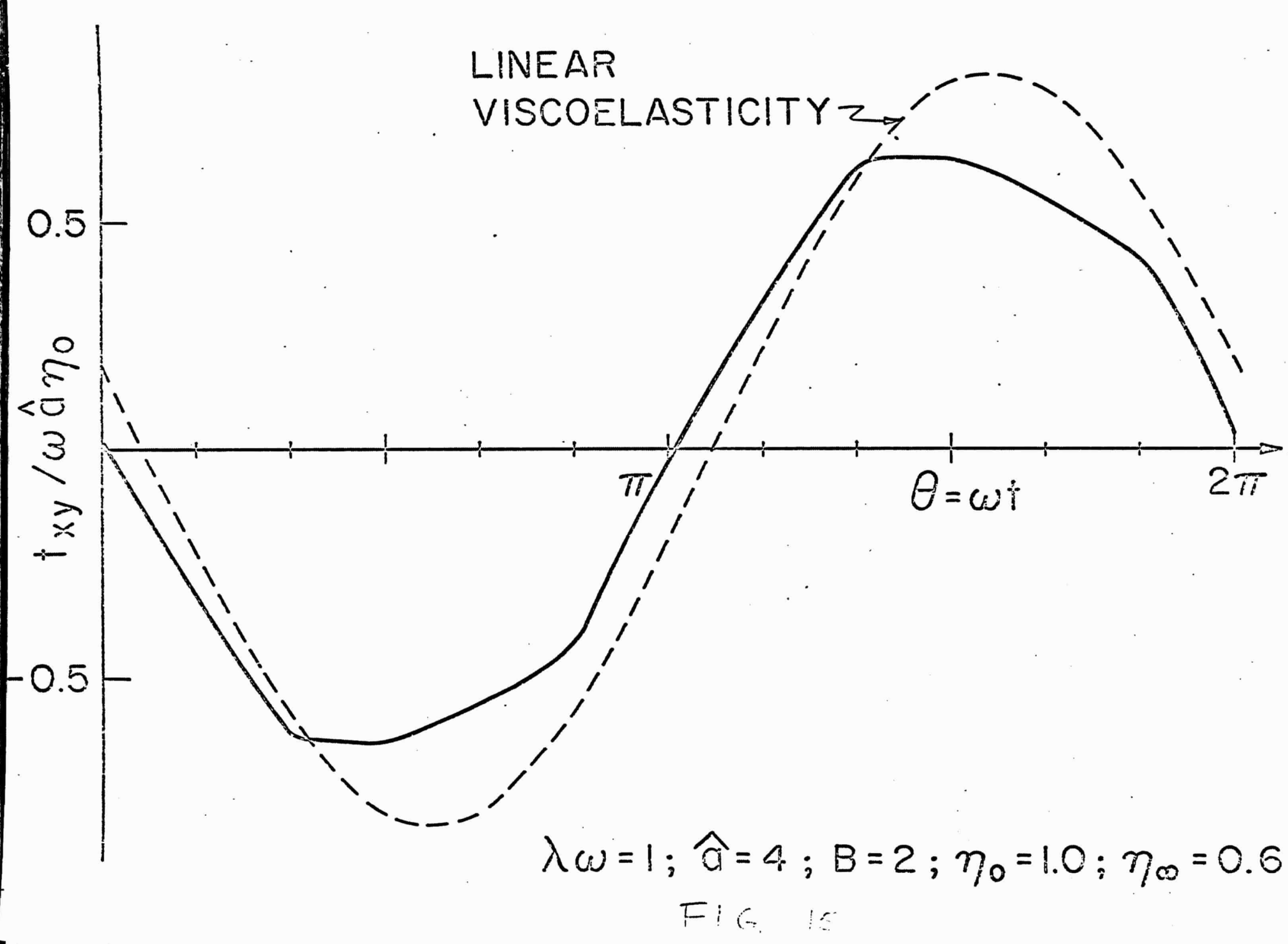
LINEAR
VISCOELASTICITY
0.5
-0.5
$t_{xy}/\omega\hat{a}\eta_0$
π
$\theta = \omega t$
2π
$\lambda\omega = 1$; $\hat{a} = 4$; $B = 2$; $\eta_0 = 1.0$; $\eta_\infty = 0.6$

FIG. 15

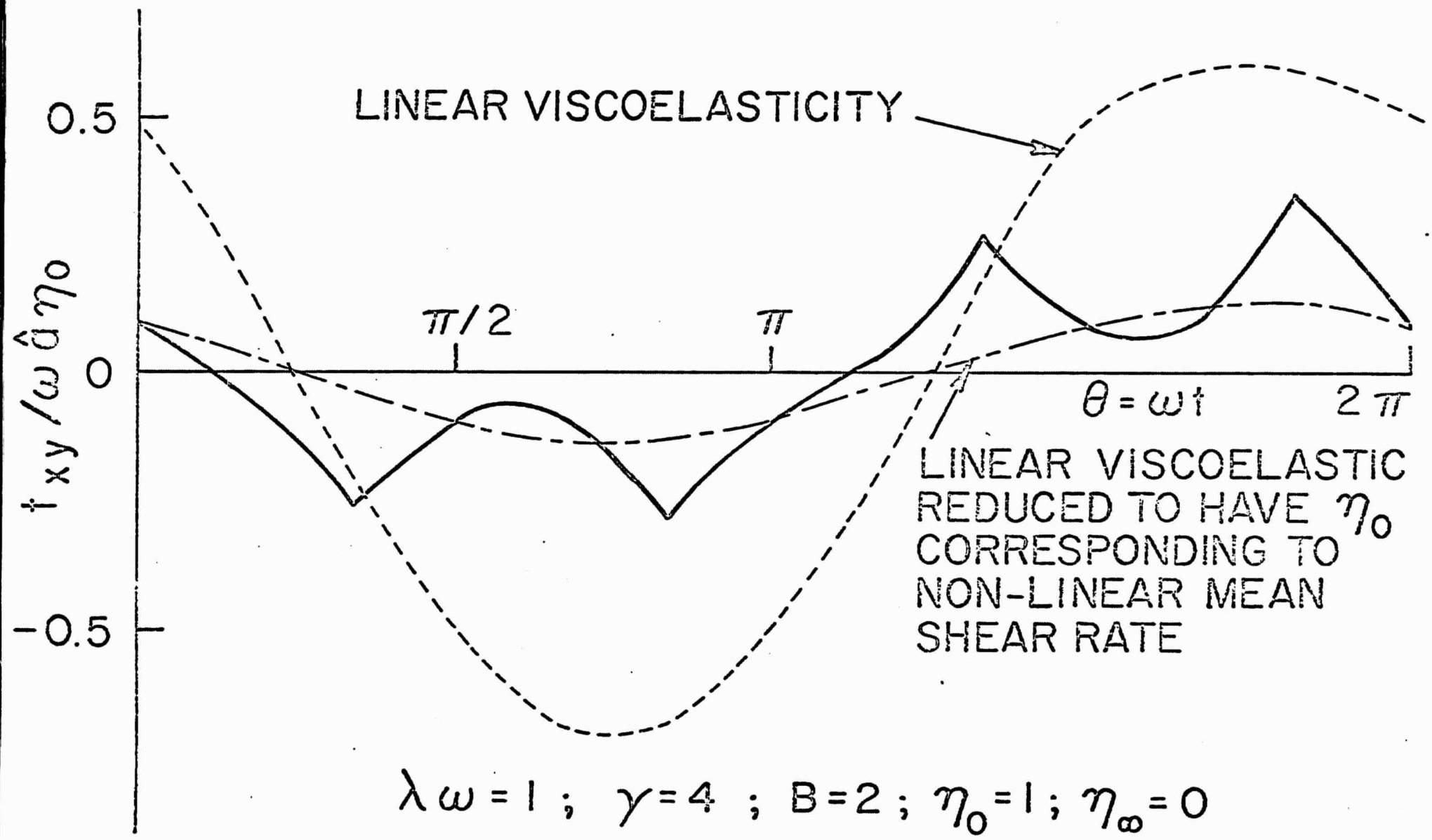

$\lambda\omega = 1$; $\gamma = 4$; $B = 2$; $\eta_0 = 1$; $\eta_\infty = 0$

FIG. 16

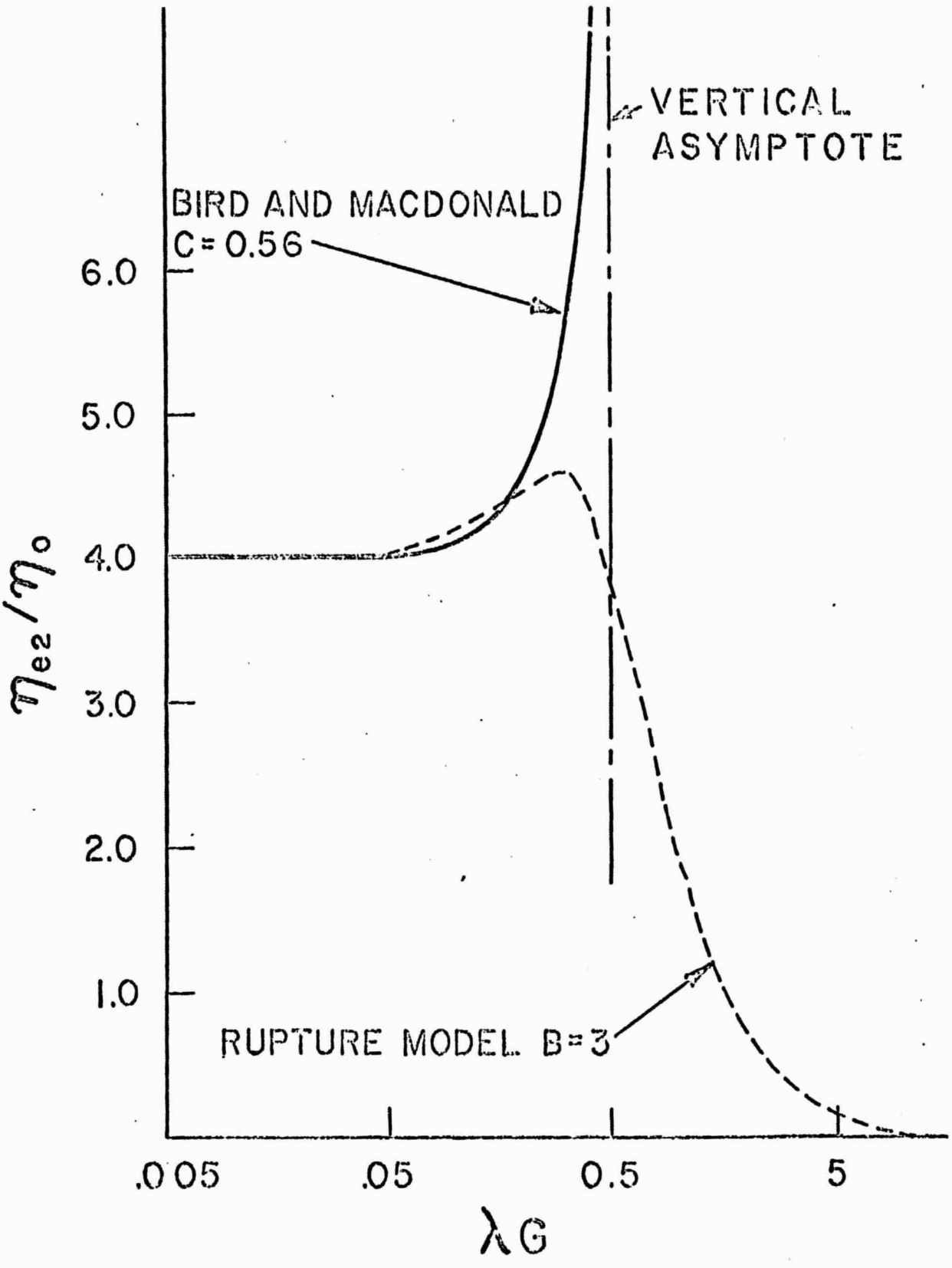
VERTICAL
ASYMPTOTE
BIRD AND MACDONALD
C = 0.56
6.0
5.0
4.0
3.0
2.0
1.0
η_{e2}/η_0
RUPTURE MODEL. B=3
.005
.05
0.5
5
λG

FIG. 17

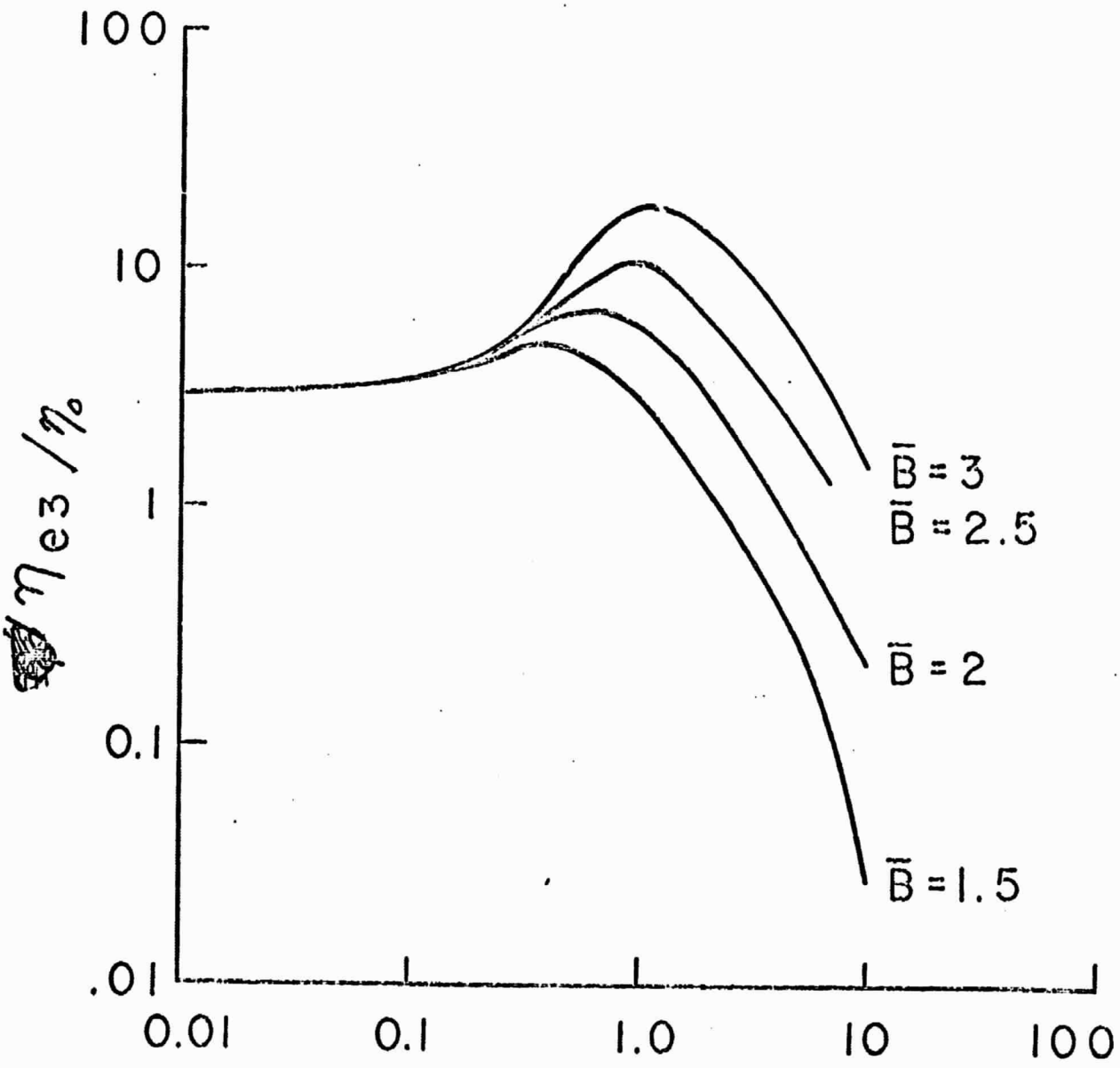
100
10
1
0.1
.01
η_{e3}/η_0
$\bar{B} = 3$
$\bar{B} = 2.5$
$\bar{B} = 2$
$\bar{B} = 1.5$
0.01
0.1
1.0
10
100
λG

FIG. 18

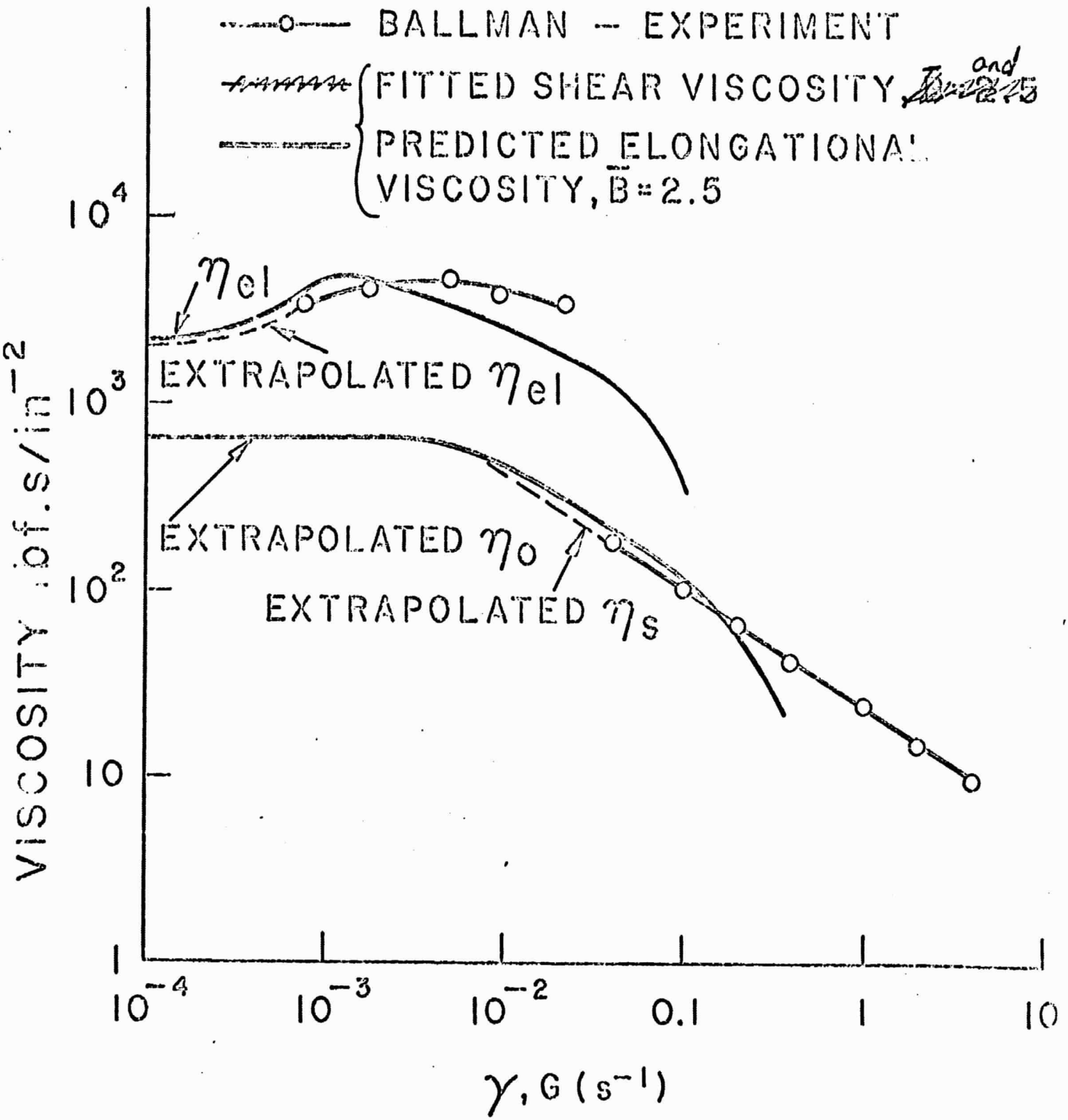
BALLMAN — EXPERIMENT
FITTED SHEAR VISCOSITY, B = 2.25 and 2.5
PREDICTED ELONGATIONAL VISCOSITY, B = 2.5
η_{el}
EXTRAPOLATED η_{el}
EXTRAPOLATED η_0
EXTRAPOLATED η_s
VISCOSITY, lbf.s/in^{-2}
10^4
10^3
10^2
10
1
10^{-4}
10^{-3}
10^{-2}
0.1
1
10
γ, G (s^{-1})

FIG. 19